

Correspondence

Operation of an Esaki Diode Microwave Amplifier*

A microwave amplifier using a germanium Esaki diode has been operated at 4.5 kmc with the following results:

Maximum stable gain	= 23 db;
Voltage gain—bandwidth product (23-db gain at a bandwidth of 20 mc)	= 2.75×10^8 ;
Effective source noise temperature (noise figure = 7 db)	= 1200°K;
Saturation power output	$\approx 1 \times 10^{-6}$ watt.

The diode peak current was 1.1 ma and the peak-to-valley ratio was 2.5.

The amplifier is shown schematically in Fig. 1. It consists of a single port cavity *A*, containing the Esaki diode *B*, which is coupled via an iris to a short section of a waveguide beyond cutoff *C*, separating it from the main propagating waveguide *D*. The incident input signal and the reflected (and amplified) output signal are separated by a low-loss circulator.

As with all regenerative amplifiers, sufficient loading must be provided to prevent oscillation from taking place. This was achieved by a dielectric plug, *E*, which, when completely inserted into the cutoff section, enables the latter to propagate. The depth of insertion is thus used to vary the external coupling of the cavity.¹

It can be shown that, for high gain, the voltage gain-bandwidth product is given by

$$\sqrt{G} \Delta f \approx \frac{1 - \frac{Q_d}{Q_c}}{\pi RC} \quad (1)$$

where Q_d/Q_c is the ratio of the power dissipated inside the cavity to that generated by the negative resistance of the diode. R and c are, respectively, the negative resistance and the capacitance of the diode. G is the power gain while Δf is the separation in cycles/second between the half-power points. The constancy of $\sqrt{G} \Delta f$ was checked at $G=23$ db and $G=17$ db. Since Q_d/Q_c in our experiment was ~ 0.5 , the measured result, $\sqrt{G} \Delta f = 2.75 \times 10^8$, represents approximately one half of the asymptotic value attainable according to (1) in the limit of strong over-coupling, $Q_c \gg Q_d$.

The effective source noise temperature T_e^2 is given by the relation

$$T_e = \frac{(\sqrt{G} + 1)^2}{G} \cdot \left[T_c \left(\frac{Q_{ex}}{Q_c} \right) + \frac{e I_0 R}{2k} \left(\frac{Q_{ex}}{Q_d} \right) \right] \quad (2)$$

where

T_c is the cavity ambient temperature;

$$\frac{Q_{ex}}{Q_c} = \frac{\text{external "Q"}}{\text{unloaded "Q"}}$$

* Received by the IRE, February 16, 1960.

¹ This scheme was first used by J. P. Gordon in a paramagnetic resonance experiment.

² T_e is related to the noise figure F by the relation

$$F = 1 + \frac{T_e}{290}$$

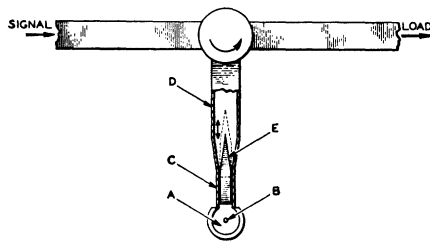


Fig. 1—A schematic view of the Esaki diode amplifier. (The symbols are explained in the text.)

is the ratio of the power lost in the cavity to that delivered to the external load;

Q_{ex}/Q_d is the ratio of the power generated by the diode to that supplied to the load;

I_0 is the dc bias current;

e is the electronic charge;

k is Boltzmann constant; and

$-R$ is the negative resistance of the diode.

The measured noise temperature of 1200°K was approximately twice as high as that expected from (2) in the limit of strong coupling where $Q_{ex} \ll Q_c$. This difference is due to the operation of the cavity near the condition of critical coupling. An increase in coupling was prevented by the amount of parasitic losses inside the cavity, which placed a limit on the maximum loading at which high gain could be obtained. Substantially lower noise temperatures are to be expected from diodes with better peak-to-valley current ratios (where lower values of $I_0 R$ can be attained), and from diodes with smaller series resistance. There is also the possibility of intrinsically lower $I_0 R$ products with other semiconductors.

The authors wish to express their gratitude to E. Dickten who fabricated and mounted the diode used in the experiment.

A. YARIV
J. S. COOK
P. E. BUTZIEN
Bell Telephone Labs.
Murray Hill, N. J.

Voltage Tuning in Tunnel Diode Oscillators*

During some recent experimental work on microwave tunnel diode oscillators, voltage tuning ranges of up to 12 per cent have been obtained by varying the operating bias of the oscillator. Power output was approximately -30 dbm.

Fig. 1 shows a curve of frequency vs voltage obtained with an oscillator using an Esaki diode, manufactured by Sony Corporation, Japan. The diode was mounted at one end of a low impedance coaxial line, as shown in Fig. 2, and the other end of the line was terminated in a matched load, across which the operating voltage was applied.

* Received by the IRE, February 29, 1960.

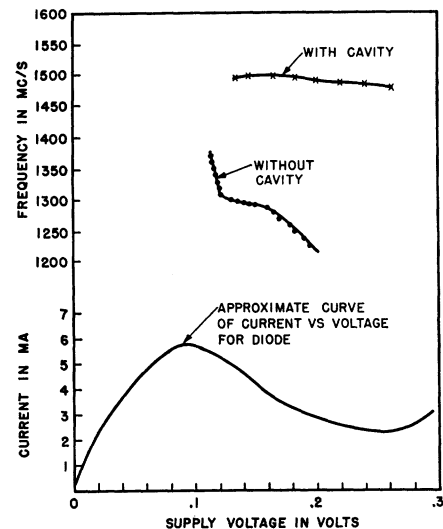


Fig. 1—Voltage tuning curves for tunnel diode oscillator.



Fig. 2—Tunnel diode oscillator (output was taken from a probe at the diode end).

The dependence of frequency on the operating potential in a voltage-controlled negative resistance oscillator is a well-known phenomenon. The mechanism is particularly clearly explained by Edson.¹ As the diode has a nominal maximum negative resistance of 25 ohms, and the impedance of the coaxial line is 20 ohms, there is quite a wide band near the resonant frequency of the diode package where the diode can oscillate.

By varying the operating voltage, the effective negative resistance of the diode at which the oscillation will reach a steady state may be varied, and thus the frequency will change. The relative amplitude and phase of the harmonics generated will also vary with supply voltage, and, as shown by Edson, this also affects the oscillation frequency. The nonlinearity of frequency vs voltage is thought to be due to resonances at the harmonic frequencies.

By adding a quarter wave re-entrant cavity in the center conductor of the coaxial line, the impedance at the oscillating frequency can be raised, resulting in more power output (approximately -15 dbm) but a voltage tuning range of only about 20 mc at 1500 mc or 1.3 per cent. Both oscillators could be tuned mechanically over a 30 per cent bandwidth with little change in output.

J. K. PULFER
Radio and Electrical
Engineering Division
National Research Council
Ottawa, Ontario, Canada

¹ W. A. Edson, "Vacuum Tube Oscillators," John Wiley and Sons, Inc., New York, N. Y.; 1953.

A Technique for Cascading Tunnel-Diode Amplifiers*

The tunnel diode can often be used as the active element in a conventional amplifier stage. It is at times desirable to cascade such amplifiers. Since the tunnel diode is a two-terminal device it does not supply the isolation of either the vacuum tube or the transistor. Thus, special techniques must be used when cascading tunnel-diode amplifiers. Such a technique is presented here. For convenience, voltage amplification will be discussed although a similar discussion could be applied to current amplification or power amplification.

Let us consider the simple tunnel-diode amplifier shown in Fig. 1. We shall assume that L_1 and L_2 are such that they act as open circuits at all frequencies of interest, while C is such that it acts as a short circuit at all frequencies of interest. The elements L_1 , L_2 , and C are used to supply direct bias. The equivalent circuit for the tunnel diode can be represented simply by a negative resistance over a wide range of frequencies. This will be done here. The equivalent circuit for this amplifier is shown in Fig. 2. The voltage gain of this circuit is given by

$$K = \frac{E_2}{E_1} = \frac{R}{R - r} \quad (1)$$

Note that K can be made as large as desired by choosing $-r$ so that $R - r$ is sufficiently small. However, stability requirements usually limit the maximum value of K . If the

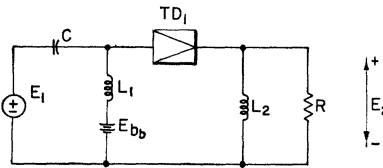


Fig. 1—A simple tunnel-diode amplifier.

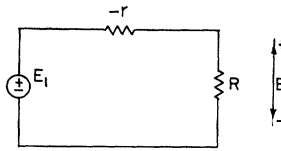
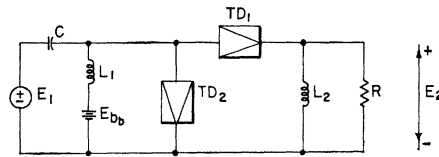
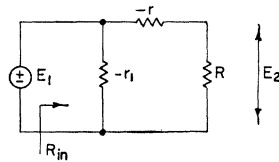


Fig. 2—The equivalent circuit for the simple tunnel-diode amplifier of Fig. 1.



(a)



(b)

Fig. 3—(a) A tunnel-diode amplifier that can be cascaded; (b) its equivalent circuit.

$$R_{in} = \frac{-r_1(R - r)}{R - r - r_1} \quad (2)$$

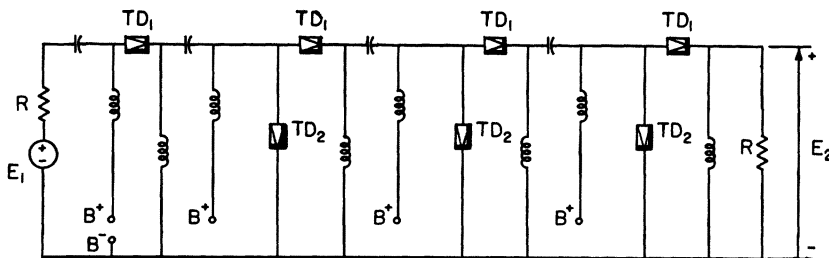
Now let us choose $-r_1$ so that $R_{in} = R$. Then solving (2) for $-r_1$, we obtain

$$-r_1 = \frac{R(R - r)}{-r} \quad (3)$$

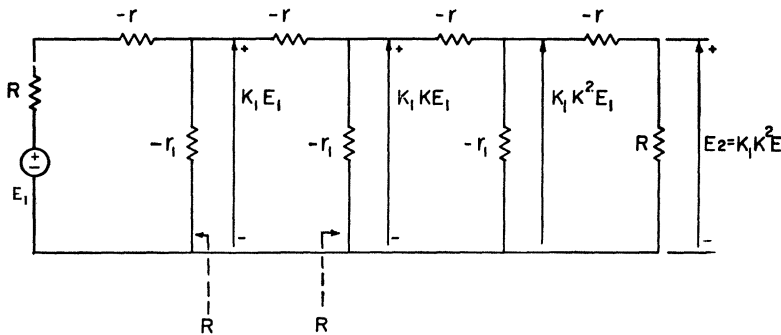
The input resistance of this circuit is now equal to the load resistance, thus this circuit may be used as the "load resistance" of a similar circuit. When several of such stages are cascaded the voltage gain of each will be $K = R/(R - r)$. The over-all gain will, of course, be the product of the individual stage gains. For instance, a typical circuit is shown in Fig. 4(a). The over-all voltage gain of this circuit is $K_1 K^2$, where $K_1 = R/(2R - r)$ is the gain of the first stage. Note that it has been assumed that the internal resistance of the signal source is not zero but is equal to the load resistor R . The equivalent circuit for this amplifier is shown in Fig. 4(b). Pertinent voltages and resistances are indicated in this equivalent circuit. The resistances are "viewed" in the direction shown by the arrow.

The previous discussion considered the cascading of amplifier stages. Actually, the circuit of Fig. 4 may be viewed as a transmission line connecting the input generator to the output load. In this case, the transmission line is made up of negative resistance elements and, hence, produces a gain rather than a loss. Note that with some minor modification this "transmission line" can start and end with shunt rather than series elements.

If impedances are placed in series with the series tunnel diodes (TD_1) and impedances are placed in shunt with the shunt tunnel diodes (TD_2), then the gain of the amplifier can be made frequency dependent. This must be done with care to insure that the amplifier will be stable.



(a)



(b)

Fig. 4—(a) A typical cascaded tunnel-diode amplifier; (b) its equivalent circuit.

P. M. CHIRLIAN
Dept. of Electrical Engineering
New York University
New York, N. Y.

* Received by the IRE, February 15, 1960.

Negative L and C in Solid-State Masers*

When a material exhibiting quantum-mechanical resonance absorption is caused to be emissive by producing an inverted population distribution—which is necessary for maser operation—the impedance behavior of the material changes in two ways: not only does the resistive component become negative to provide gain, but the dependence of the reactive component on frequency reverses sign. This second property can be used to obtain gain and bandwidth performance that exceeds the limitations imposed by conventional network analysis. For amplifier design calculations, it is convenient to represent this fact by an equivalent circuit. For example, the permeability of a crystal in the neighborhood of a sharp electron paramagnetic resonance (for a Lorentz-shaped line) is of the form

$$\mu = \mu_0 \left(1 - \frac{j\chi_{\max}''}{1 + jT_2\Delta\omega} \right) \quad (1)$$

where χ_{\max}'' is the peak value of the absorptive component of complex susceptibility, and T_2 is the reciprocal linewidth. This relation may be represented by the equivalent circuit shown in Fig. 1 with $G=1/(\mu_0\chi_{\max}''\omega_0)$, and $jB=(jT_2\Delta\omega)/(\mu_0\chi_{\max}''\omega_0)$. When the population is inverted, the permeability becomes

$$\mu = \mu_0 \left(1 + \frac{j\chi_{\max}''}{1 + jT_2\Delta\omega} \right),$$

for which the corresponding circuit becomes that shown in Fig. 2, in which all symbols are taken as positive. For a Gaussian-shaped line, the expressions are an approximation that is only valid in the center of the line, but the general conclusions are true.

This result is obtained by solving the equation of motion for the system in question,¹ and it can be readily observed experimentally. When the crystal is incorporated in a cavity resonator, an appropriate circuit suggested is that shown in Fig. 3. When the negative terms in this circuit are large compared with the positive terms (a situation that represents a strong paramagnetic resonance and a large filling factor), the circuit shown in Fig. 4 is suggested. The normal C'' and L'' are used to compensate for the negative L and C of the electron-spin resonance, to achieve increased bandwidth. The circuit of Fig. 4 represents two cascaded cavities with an inverted paramagnetic crystal in the second. In order to achieve significant improvement, L' must be small. The criterion suggested by stored-energy implications is

$$LG \leq \frac{C}{G} \quad (2)$$

* Received by the IRE, March 2, 1960. This work was supported in part by the U. S. Army (Signal Corps), the U. S. Air Force (Office of Scientific Research, Air Research and Development Command), and the U. S. Navy (Office of Naval Research).

¹ F. Bloch, "Nuclear induction," *Phys. Rev.*, vol. 70, pp. 460-474 (see sec. III); October 1 and 15, 1946; R. Karplus and J. Schwinger, "Saturation in microwave spectroscopy," *Phys. Rev.*, vol. 73, pp. 1020-1026 (see eq. 23); May 1, 1948.

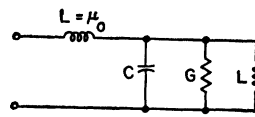


Fig. 1.

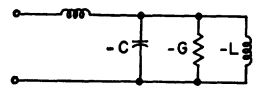


Fig. 2.

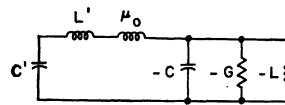


Fig. 3.

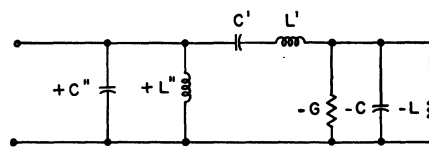


Fig. 4.

and this has been verified by direct calculation.

If a filling factor of 1 is obtained in the active cavity, (2) reduces to

$$\chi_{\max}'' \geq \frac{1}{\omega_0 T_2}, \quad \text{or} \quad \chi_{\max}'' \geq \frac{\Delta\omega_0}{\omega_0} \quad (3)$$

where $\Delta\omega_0$ is the full width of the paramagnetic-resonance line. This condition is just about met for "pink" ruby at 9 kmc and at 4.2°K, for which, under typical experimental conditions, $\chi'' \approx 0.01$, and $\Delta\omega_0/\omega_0 \approx 0.005$. Cavity losses, which are usually small under these conditions, were ignored in our analysis. A maser in which these phenomena are utilized has been constructed by Goodwin and Moss.²

The gain-bandwidth theory of Fano³ can be extended to the negative L and C situation. In the high-gain limit, with a single maser crystal, it gives

$$\frac{1}{\pi} \int \ln \mathcal{G}^{1/2} d\omega = \Delta\omega_0 \left[\left(1 + \frac{3\chi_{\max}''\omega_0}{\Delta\omega_0} \right)^{1/3} - 1 \right] \quad (4)$$

where the integral is over the amplifier bandwidth, and $\mathcal{G}^{1/2}$ is the voltage gain of the cavity maser as a function of frequency.

Increasing the spin concentration augments the effect by increasing χ'' , as long as the linewidth $\Delta\omega_0$ does not increase also. Raising the operating frequency augments the effect for a given sample by increasing both χ'' and $\omega_0/\Delta\omega_0$. Lowering the temperature, of course, also helps.

² F. E. Goodwin and G. E. Moss, Hughes Aircraft Co., Research Labs., Culver City, Calif., private communication; November 12, 1959.

³ R. M. Fano, "Theoretical limitations on the broadband matching of arbitrary impedances," *J. Franklin Inst.*, vol. 249, pp. 57-84; January, 1950; vol. 249, pp. 139-154; February, 1950.

The presence of the negative L and C terms does not materially change the performance of a typical traveling-wave maser because the circuit is too broad-band to introduce sufficient compensating reactance.

Incidentally, these negative L and C properties do not appear in parametric amplifiers. The broad-banding procedures discussed by Seidel and Herrmann,⁴ for example, are of a more conventional type.

R. L. KYHL

Dept. of Electrical Engineering and
Research Laboratory of Electronics
Mass. Inst. Tech.
Cambridge, Mass.

⁴ H. Seidel and G. F. Herrmann, "Circuit aspects of parametric amplifiers," 1959 IRE WESCON CONVENTION RECORD, Part 2, pp. 83-91.

Parametric Oscillatory and Rotary Motion*

The semiconductor parametric amplifier belongs to a more general class of devices, in which one or more parameters in the underlying integro-differential equation are periodic time functions. In principle, the reactance variation may equally well be accomplished by ferromagnetic means, so that the inductance becomes a periodic function. The conditions for oscillations are

$$L \frac{di}{dt} + i \frac{dL}{dt} + Ri + \frac{1}{C} \int idt = 0, \quad (1)$$

$$C \frac{dv}{dt} + v \frac{dC}{dt} + Gv + \frac{1}{L} \int vdt = 0. \quad (2)$$

Here (2) is the better-known equation, pertaining to a variable-capacitance amplifier with $\beta A = 1$. The second term identifies the opportunity of amplification, offered with C varied at twice signal frequency. The capacitance variation frequency is the pump frequency, at which the capacitance is reduced on every half-cycle of the signal voltage wave, thus giving off energy to the rest of the system. This is the way the stimulance is injected, which in an amplifier almost, but not quite, takes care of the dissipation.

The writer has undertaken to investigate parametric devices with mechanical rather than electrical input signal.¹ Variable inductance devices at low frequency proved to offer the easiest approach, and several mechanical oscillators with equal pump and signal frequencies were successfully constructed. Thus, "the world's simplest servosystem" emerged, with the model adjusted for $\beta A < 1$. With the aid of the second term in (1), $i dL/dt$, a small mechanical displacement x was turned into a larger mechanical one, associated with much more power, and it is only logical to expect that a similar servosystem can be designed in accordance

* Received by the IRE, March 1, 1960.

¹ H. P. Knauss and P. R. Zissel, "Magnetically maintained pendulum," *Amer. J. Phys.*, vol. 19, pp. 318-320; May, 1951.

with (2). Thus a narrow-frequency-range oscillating reed, telephone, or loudspeaker design may be based on either equation, not to mention other devices of this general nature with or without supporting active elements, such as switching transistors.

With the aid of a Mathieu-Hill type of equation solution, it can be shown that the term $i dL/dt$ yields a double-valued force function, the explanation for the easily demonstrated fact that sustained oscillations are obtained. To show that nonlinearity is not essential, an additional small-signal model was built without iron, and proved to oscillate. Since in the solution of the equation, the double-valued force function is independent of the sign of the displacement x , the association of the stimulance part of the force function with $-x$ is by no means unique; it could just as well be $+x$. To prove this theoretical point, predicting rotational motion, the "electronics motor" in Fig. 1 was constructed, and true enough it rotated. The favored speed of the model is about 200 rpm. The effect can be enhanced if a switching transistor amplifier of time constant T and with $Z_i \gg Z_o$ is attached, for example, as indicated by the dotted lines. The transistor amplifier is not essential to the operation, nor is the capacitor C_1 . This capacitor was introduced because it made the circuit approach resonance conditions, and thus accept a heavier current. It yields the frequency $1/2\pi\sqrt{L_1 C_1}$, or which is lower than the lines frequency. Thus the slope $di/d\omega$ is negative, so that the stimulance part of the force function pertaining to $i dL/dt$ is aided by the force function due to $di/d\omega$, in which $\omega = 2\pi f$, with the particular value $f = 60$ designating lines frequency.

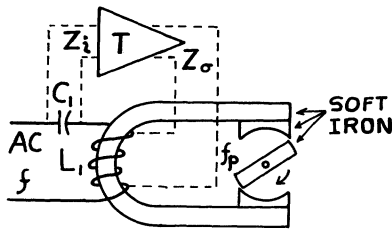


Fig. 1—Principle of the parametric motor. The rotor spins around in either direction, although there are no contacts, no rotor winding, no magnets, no rotational field, and no synchronous speed.

HARRY E. STOCKMAN
Dept. of Elec. Engrg.
Merrimack College
North Andover, Mass.

A Transverse-Field Traveling-Wave Tube*

Recently there has been an urgent interest in traveling-wave parametric amplifiers which utilize an electron beam as the reactive element. One such amplifier which has achieved very-low-noise performance has

been described by Adler *et al.*¹ The amplifier uses the fast electron cyclotron wave as the signal and idler modes and a traveling high-frequency electric quadrupole field as the pump mode. In the Adler Tube the pump frequency is set equal to twice the cyclotron frequency of the electrons and the phase velocity of the pump wave is infinite.

There is also a related class of beam-type parametric amplifiers in which the pump mode is at an arbitrarily low frequency including dc and the pump phase velocity is finite including zero. The idler mode is a slow cyclotron wave. These amplifiers are not characterized by extremely low-noise performance, but have other interesting properties as has been shown by Gordon *et al.*² It is the purpose of this paper to present preliminary experimental results on an amplifier using a static spatially-varying electric quadrupole field to achieve amplification of the fast cyclotron wave.

The interaction in the static quadrupole field can be understood by reference to Fig. 1 in which an electron in the phase appropri-

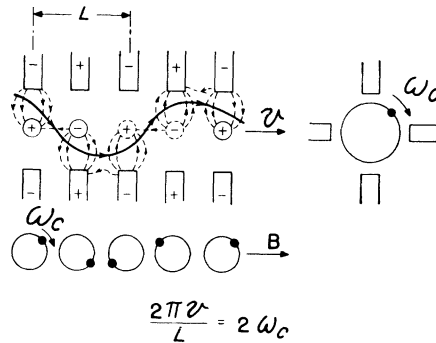


Fig. 1—The energy-gain mechanism.

ate to energy gain is shown. The drifting electron gains rotational energy as it loses drift energy; the quadrupole fields merely serving to deflect the electron. No energy is transferred from the quadrupole fields to the beam. It can be seen, also, that the synchronism condition requires that $2\omega_c = 2\pi v/L$, ω_c being the cyclotron frequency, v the drift velocity and L the periodic spacing of the quadrupole fields. Thus, the drifting electrons experience an apparent pump field of frequency $2\omega_c$.

As in the Adler device, an exponential growth of the orbit occurs which, coupled with a phase focusing induced by the quadrupole fields, leads to a net increase in the kinetic power of the fast cyclotron wave. Since no power is supplied by the pump fields and the drift velocity of the beam is decreased, it follows that the idler wave is a slow wave. Hence the zero pump frequency amplifier also may be compared to the conventional traveling-wave tube in which the corresponding "fast" wave is the electromagnetic wave carried by the slow-wave circuit while the "idler" wave is the slow space-charge wave.

¹ R. Adler, G. Hrbek, and G. Wade, "The quadrupole amplifier, a low-noise parametric device," *Proc. IRE*, vol. 47, pp. 1713-1723, October, 1959.

² E. I. Gordon, S. J. Buchsbaum, and J. Feinstein, "A Transverse Field Amplifier Employing Cyclotron Resonance Interaction," paper presented at the Seventeenth Conference on Electron Tube Research, Mexico City, Mex.; June, 1959.

The gain in the quadrupole fields is given by

$$G = 20 \log \cosh g V_q \text{ (db)} \quad (1)$$

in which V_q is the dc voltage applied to the quadrupole plates and g is a geometrical factor proportional to the number of quadrupole sections. Fig. 2 shows the observed

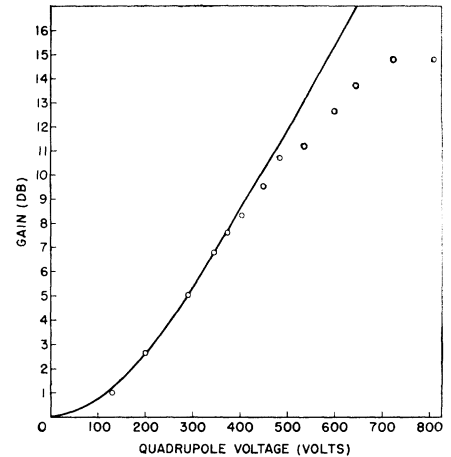


Fig. 2—Gain as a function of quadrupole.

gain minus the insertion loss as a function of the quadrupole voltage with the beam at the synchronous voltage. The solid line is the curve predicted by (1) in which the value of the constant g has been adjusted. The value of the constant is 30 per cent higher than the value calculated from knowledge of the quadrupole geometry. The experimental points depart considerably from the predicted curve for gains above 8 db. At this point, interception on the quadrupole begins. This results from a defect in the electron gun which introduces up to twenty volts of rotational energy onto the beam and is not inherent in the device. The deficit in gain is a result of the interception and the departure from the synchronous condition resulting from the decrease in beam voltage of those electrons with large rotational energy. The beam voltage and current are 800 volts and 2 ma, respectively. The quadrupole structure has a periodicity of 0.25 cm with an inner diameter of 0.20 cm and has 10 periods. The couplers are ridged waveguide cavities with a center-band frequency of 3.25 kmc and a bandwidth of 2 per cent.

A major advantage of the device is the fact that after the fast-wave energy is stripped from the beam in the output coupler, the remaining excitation on the beam is the slow idler wave. Thus, the spent electrons are monoenergetic and can be collected at close-to-cathode potential. As a result, the efficiency of the device can be very high.

No noise measurements have been made as yet, and although the device is not expected to have the extreme low-noise performance of the high-frequency-pumped amplifier, there is every reason to believe that it will compete with the more conventional traveling wave tubes in this respect.

E. I. GORDON
Bell Telephone Labs., Inc.
Murray Hill, N. J.

* Received by the IRE, March 7, 1960.

WWV and WWVH Standard Frequency and Time Transmissions*

The frequencies of the National Bureau of Standards radio stations WWV and WWVH are kept in agreement with respect to each other and have been maintained as constant as possible with respect to an improved United States Frequency Standard (USFS) since December 1, 1957.

The nominal broadcast frequencies should, for the purpose of highly accurate scientific measurements, or of establishing high uniformity among frequencies, or for removing unavoidable variations in the broadcast frequencies, be corrected to the value of the USFS, as indicated in the table below.

WWV FREQUENCY WITH RESPECT TO U. S. FREQUENCY STANDARD	
1960 March 1600 UT	Parts in 10 ¹⁰ †
1	-146
2	-146
3	-146
4	-146
5	-146
6	-145
7	-145
8	-145
9	-145
10	-145
11	-145
12	-144
13	-144
14	-144
15	-144
16	-144
17	-144
18	-145
19	-144
20	-144
21	-144
22	-144
23	-144
24	-144
25	-144
26 §	-144
27	-147
28	-147
29	-147
30	-146
31	-146

† A minus sign indicates that the broadcast frequency was low.

§ On March 26 the frequency was decreased 3 × 10⁻¹⁰.

The characteristics of the USFS, and its relation to time scales such as ET and UT2, have been described in a previous issue,¹ to which the reader is referred for a complete discussion.

The WWV and WWVH time signals are also kept in agreement with each other. Also they are locked to the nominal frequency of the transmissions and consequently may depart continuously from UT2. Corrections are determined and published by the U. S. Naval Observatory. The broadcast signals are maintained in close agreement with UT2 by properly offsetting the broadcast frequency from the USFS at the beginning of each year when necessary. This new system was commenced on January 1, 1960. The last time adjustment was a retardation adjustment of 0.02 s on December 16, 1959.

NATIONAL BUREAU OF STANDARDS
Boulder, Colo.

* Received by the IRE, April 25, 1960.
¹ "United States National Standards of Time and Frequency," PROC. IRE, vol. 48, pp. 105-106; January, 1960.

Correction to "On the Regenerative Pulse Generator"*

Viktor Met, author of the above Correspondence, which appeared on pages 363-364 of the March, 1960, issue of PROCEEDINGS, has advised the Editor that the drawings of Figs. 2 and 3 were preliminaries, and should have been replaced with ones submitted at a later date. The revised figures are reproduced herewith.

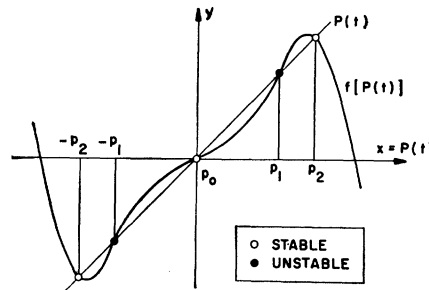


Fig. 2—Graphical solution of the nonlinear difference equation for a fifth-order nonlinearity.

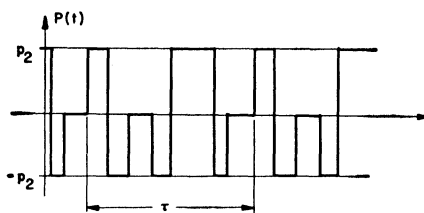


Fig. 3—Step-function, representing the general steady state solution.

* Received by the IRE, March 17, 1960.

Anomalous Reverse Current in Varactor Diodes*

While working on parametric amplifiers and harmonic generators using Varactor diodes, an interesting phenomenon was noticed concerning the direction of average diode current flow when a high-frequency pump source was applied. An appreciable reverse current was measured for dc bias voltages very much closer to forward conduction than to reverse breakdown. Measurements show that the instantaneous diode voltage is not even required to reach the dc breakdown value, and that this abnormal breakdown occurs only when the voltage during the positive-going half cycle is sufficiently large to swing into the forward conduction region. A plausible explanation of this phenomenon is that the large number of

minority carriers injected during the forward half cycle are multiplied through collision ionization on the reverse half cycle, yielding a net negative current.¹ This occurs only at high frequencies because the voltage can swing negative before an appreciable number of injected carriers are lost through recombination or diffusion to the junction.

At X band, the effect is quite pronounced with a Bell Laboratories type Si 43 Varactor whose reverse characteristic is "hard" (less than 1-μa reverse current flows until breakdown occurs at -10.5 volts). An applied X band signal causes a reverse current of 20 μa at only -0.5 volt bias, although the diode characteristic is such that forward current of several microamperes occurs at +0.6 volt. For a slightly more positive value of bias, the current passes through zero and becomes positive. The dc bias at which the transition from forward to reverse current occurs was plotted as a function of frequency (Fig. 1). Since the ac drive varied

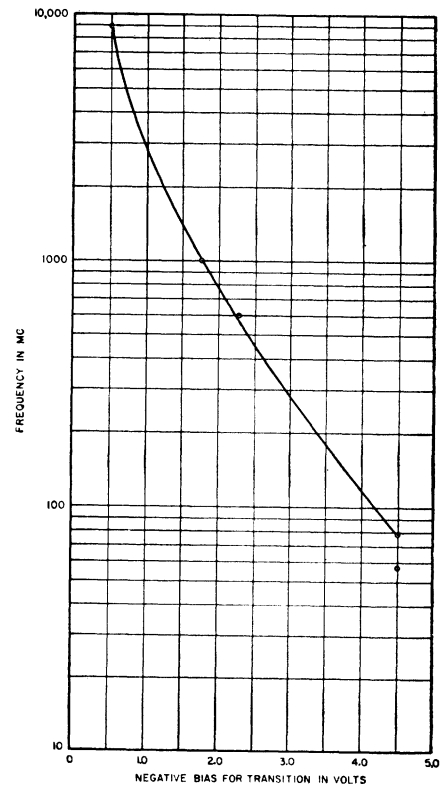


Fig. 1—Trend of effect vs frequency.

over the frequency range, this curve should be regarded only as illustrating a trend. The anomalous effect is seen to be most pronounced for the highest frequencies and disappears below about 60 mc for the above diode. This frequency region agrees with the minority carrier lifetime of 0.05 μsec² for these diodes. Since the effect was small or negligible below several hundred megacycles, a direct observation of diode waveforms could not be made.

¹ Suggested by A. Uhlir, Jr., in a conversation held at Airborne Instruments Lab.
² "Crystal Rectifiers," Bell Telephone Labs., Ninth Interim Tech. Rep., Signal Corps Contract DA-36-039-sc-5589; October 15, 1956.

* Received by the IRE, October 26, 1959. This work was supported under Air Force Contract AF30(602)-1854.

There are at least two explanations which may describe the above phenomena. One explanation requires that the ac signal be large enough to swing into both forward conduction and dc breakdown. Rectification about the forward characteristic should be poor because of minority carrier storage, and thus breakdown current should counterbalance the forward current at bias levels closer to forward conduction. This effect would be aided by the asymmetry of the waveform of voltage across the diode, which is peaked in the negative direction because of the shape of the C-V curve.

The second explanation is that the voltage does not reach the dc breakdown value, but at high frequencies some new mechanism occurs causing reverse current to flow at a voltage less than the normal dc breakdown voltage. To determine which explanation is correct, we have measured the voltage across the diode under conditions when the anomalous behavior was observed. This was done by two methods. The first method involved determining the amplitude of the various frequency components of the voltage across the diode by the use of a slotted line and reconstructing the waveform under the most pessimistic assumptions about phase. If the relative phases were such that all the peaks added in the negative direction, the maximum reverse voltage would only be 6.6 volts. This is considerably less than the value of 10.5 volts at which dc breakdown occurs.

At this point, we must mention the difference between the voltage we measure at the diode terminals and that which exists at the junction. The diode lead inductance is resonant with the junction capacitance from 3 to 4 kmc depending on the bias. The fundamental frequency was made low enough (470 mc) so that even at the third harmonic the parasitic elements introduce a negligible discrepancy.

For a second independent measurement to determine whether the diode voltage reaches dc breakdown, a high-frequency peak reading voltmeter (HP410B) was mounted in 50-ohm line directly in front of the diode and its coaxial mount. The meter response was flat to the fourth harmonic of the 185-mc signal used here. By reversing the diode and bias polarities with respect to the meter, both forward and reverse peaks were measured. They were +1.4 volts and -7.3 volts respectively. Again we see that the reverse peak does not reach the breakdown level.

Additional enlightenment as to the nature of the reverse conduction process results from a plot of average diode current vs bias for a fixed value of ac drive. (See Fig. 2.) The curve shown is for 370 mc. Similar results were found at other frequencies. The current is seen to be continuous through zero, indicating both forward and reverse current even at small bias levels. After switching from negative to positive it returns to zero for a range of bias values midway between the forward and reverse portions of the dc characteristic. This indicates that the voltage swing is too small to enter either conduction region when biased midway. Therefore, the negative current at small bias levels is not due to a large signal

entering dc breakdown, but seems to depend upon forward current being drawn during part of the cycle. A further increase in bias results in breakdown current at -5.8 volts, indicating an ac amplitude of 4.7 volts. When this is added to the bias (2.8v) for the first crossover through zero, negative current is seen to be generated when the instantaneous voltage reaches -7.5 volts.

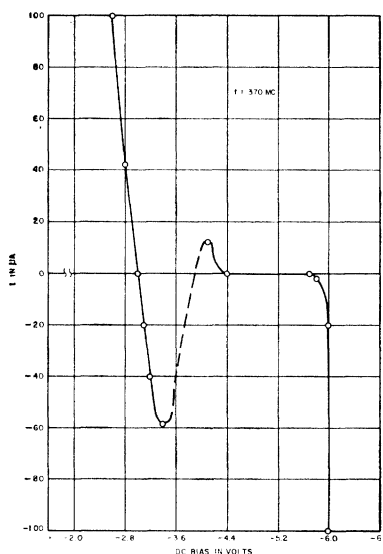


Fig. 2—Average diode current vs dc bias with ac drive (Si-43 No. 33).

The dashed portion of the curve denotes an unstable region, the operating point flipping from one extreme to the other. When biased in this region, a relaxation oscillation existed between these points at about 1 cps.

It should be noted that the circuits used have no structures tuned near the operating frequency, so that the variation of current with bias is not due to resonance effects involving the diode capacitance. The bias lead was suitably bypassed to ac.

Following the high-frequency experiments with the BTL Varactor diodes, the phenomenon was reproduced at low frequencies (15 mc) with a Hoffman 1N138 diode for which the lifetime was measured as about 1 μ sec. The ratio of lifetime to RF period is seen to be of the same order of magnitude as in the high-frequency experiment. In addition, the breakdown mechanism is known to be of the avalanche type since this diode also exhibits the random pulse phenomenon described by McKay.³ An oscilloscope verifies that the voltage is not required to reach dc breakdown, although the difference is not as great as in the high frequency case. A curve of average current vs diode bias similar to that of Fig. 2 was obtained, where the crossover through zero occurs at about -9 volts bias and the dc breakdown voltage is -27 volts.

It seems reasonable to conclude then

³ K. G. McKay, "Avalanche breakdown in silicon," *Phys. Rev.*, vol. 94, pp. 877-884; May, 1954.

that at RF periods which are short compared with the minority carrier lifetime, the carriers injected during the forward half cycle are multiplied through collision ionization on the reverse half cycle, resulting in a net reverse current. From the three high-frequency experiments presented, the maximum reverse voltage for anomalous current is about 7 volts. McKay has plotted the multiplication factor M vs V/V_b for a linearly graded silicon junction diode, where V_b is the breakdown voltage. For $V_b=10.5$, $V/V_b=0.7$, and the multiplication factor is about 2. Although this is not too much multiplication, the injected carriers represent a large increase in minority carrier density over the steady state level (of the order of 10^6). As a result, even a multiplication of two may yield considerable reverse current.

Conclusions have not yet been reached concerning the magnitude of the effects of this phenomenon on parametric amplifiers and harmonic generators, but it would seem to limit the voltage swing short of forward conduction under the penalty of an additional loss mechanism and some additional noise (even though the net dc current were zero, noise generated on the forward and reverse half cycles would degrade the noise figure of an amplifier). Operation in the nonconductive region between breakdown and forward conduction would avoid this effect, but considerable nonlinearity is probably lost by not driving into the forward region.

The author wishes to thank J. C. Greene, Dr. B. Salzberg and E. W. Sard for helpful discussions and suggestions.

K. SIEGEL
Airborne Instruments Lab.
Melville, N. Y.

Relativity and the Scientific Method*

The recent PROCEEDINGS article by J. R. Pierce¹ has triggered considerable adverse comment² on Einstein's Theory of Relativity. In the maze of detail which was discussed, one very important principle was all but forgotten, *i.e.*, the operation of the scientific method.

The objective of physical science is to provide a theoretical basis for interpretation of the observed behavior of nature. Observations are thus the final and conclusive arbiter of the "correctness" of any physical theory. It follows that a theory may never be "proved," since it is impossible to perform *all* experiments. Conversely, if such proof were possible, there would be no more

* Received by the IRE, October 22, 1959.

¹ J. R. Pierce, "Relativity and space travel," *Proc. IRE*, vol. 47, pp. 1053-1061; June, 1959.

² H. L. Armstrong, "Comment on relativity and space travel," *Proc. IRE*, vol. 47, p. 1778; October, 1959.

need for the theory itself since the purpose of any theory is to predict the outcome of new experiments. The success of a theory may thus be judged by the manner in which it fulfills this objective. In contrast, only one physical observation is required to disprove a theory. If it can be shown that a prediction of the theory is in clear contradiction to the behavior of nature as observed by a well-performed experiment, the theory must be discarded.

If we are to retain our present concepts of the scientific method, we should treat the Theory of Relativity as any other theory. No amount of belief or disbelief and no lengthy emotional expression of philosophy will substitute for a careful analysis of the observed physical facts in relation to the predictions of the theory. To date, a great number of results predicted by the Theory of Relativity have been experimentally verified. No case of clear contradiction has yet been found. Whether the theory in its present form will continue to enjoy such remarkable success indefinitely is not the subject under discussion here. Few scientists today would be willing to attest to the infallibility of any theory. However, until now the Theory of Relativity has stood the test of many critical experiments which any potential critic would do well to ponder, and until such an experiment demonstrates a clear contradiction, the critic should content himself with devising new experiments.

Irrespective of the eventual outcome of experimental work, the Theory of Relativity will remain the remarkable contribution of a remarkable man and a monument to the ability of the scientific method to bring understanding to an area where there was none.

C. A. MEAD
Calif. Inst. of Tech.
Pasadena, Calif.

A Simple General Equation for Attenuation*

The familiar equations for the attenuation of various kinds of transmission media all involve two basic kinds of dependencies. One is the intrinsic electrical properties of the conductors and dielectric; the other is the geometric configuration and scale of the cross section. It may not be generally appreciated that the attenuation of most of the media in which the waves are guided by conductors can be expressed by a single simple equation in which the two kinds of dependencies just mentioned are represented by separate and distinct coefficients. Once the equation is written, its coefficients may be readily evaluated by comparison with the usual equations for those cases for which the wave equations have been solved, or by correlation with experimental data. We be-

lieve this concept of a general equation is interesting, and that the equation itself is of considerable engineering usefulness.

One of the writers, Szekely, has produced a mathematical proof, using perturbation techniques, that the equation presented is indeed general and applies to all transmission systems having conducting surfaces parallel to an axis of a general orthogonal curvilinear coordinate system, along which the waves are propagating and in which the wave equations are separable. The proof will not be given here. It is based, however, on the assumption of good conductors and good dielectric materials. The equation applies, for example, to the attenuation per unit length of wire pairs, of coaxial conductors, of all transmission modes of waveguides of any shape of cross section, of strip lines, etc. It even applies to such structures as conical horns if the attenuation is expressed in nepers or decibels per unit length, per unit solid angle.

The attenuation per unit length of any transmission medium in the class just defined is given by

$$\alpha = \frac{M \frac{\sqrt{f}}{a} \left[A + B \left(\frac{f_c}{f} \right)^2 \right] + D}{\sqrt{1 - \left(\frac{f_c}{f} \right)^2}}, \quad (1)$$

where:

D = constant depending only on the intrinsic properties of the dielectric,

M = constant depending only on the intrinsic properties of the dielectric and of the conducting material,

A, B = constants depending on the configuration (but not the scale) of the cross section, and on the transmission mode,

a = a selected linear dimension of the cross section specifying its size or scale, all other dimensions having fixed ratios to a ,

f = transmitted frequency, and

f_c = cutoff frequency of the particular transmission mode on the given medium.

The constant D accounts for that part of the attenuation that is due to dissipation in the dielectric. In many cases where the dielectric is air or some other gas, this may be neglected. The remainder of this equation, representing the attenuation due to dissipation in the conductors, can be written in a normalized form:

$$\alpha_m \cdot a^{3/2} = \frac{M \sqrt{af} \left[A + B \left(\frac{f_1}{af} \right)^2 \right]}{\sqrt{1 - \left(\frac{f_1}{af} \right)^2}}. \quad (2)$$

where $f_1 = af_c$.

A plot of $(\alpha_m \cdot a^{3/2})$ vs (af) gives one curve that is applicable to any scale of cross section, for a given medium of given shape of

cross section and a given mode of transmission.

To apply (1) to a particular case, it is necessary to know the values of M, D, A, B and f_1 . Since M and D depend only on the conducting and dielectric materials, they can be determined once for all transmission media employing particular materials, say copper and air. Their values are given by

$$D = \frac{\eta\sigma}{2} \quad (3)$$

$$M = \frac{1}{\eta} \sqrt{\frac{\pi\mu_m}{\sigma_m}}. \quad (4)$$

In these,

$\eta = \sqrt{\mu/\epsilon}$ = intrinsic impedance of the dielectric, where μ and ϵ are the absolute permeability and dielectric constant of the dielectric,

μ_m = permeability of the conducting material,

σ = conductivity of the dielectric, and

σ_m = conductivity of the conducting material.

For a vacuum and substantially for gases, $\eta = 120\pi = 377$ ohms. For dielectrics having a different dielectric constant than that of a vacuum, $\eta = 377/\sqrt{\epsilon_r}$, where ϵ_r is the relative dielectric constant.

It shall be noted that at frequencies well above cutoff, the portion of the attenuation constant caused by a lossy dielectric is very nearly a frequency independent constant, ($\alpha_D \cong D = \frac{1}{2}\mu\sigma$); this is true for any geometric configuration, scale of cross section, or mode of transmission, provided that the conductance of the dielectric is constant and small. (In some dielectrics such as paper in paper-insulated telephone cables, σ appears to be a function of frequency.)

If rationalized MKS units are used, the attenuation given by (1) will be in terms of nepers per meter. Obviously, the attenuation may be converted to other units by multiplying M and D by suitable factors. Table I gives some values of M for copper conductors ($\sigma_m = 58 \times 10^6$ mhos per meter) and air dielectric, corrected for several combinations of units.

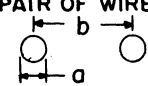
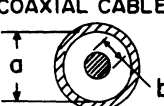
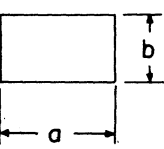
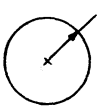
TABLE I
VALUES OF M FOR COPPER CONDUCTORS
AND GAS DIELECTRIC

α	a	f in cps.	f in KMC/sec.
Nepers/meter	cm	69.1×10^{-9}	2.19×10^{-3}
db/meter	cm	600×10^{-9}	19×10^{-3}
db/ft	inches	72.1×10^{-9}	2.28×10^{-3}
db/mile	inches	0.38×10^{-3}	12

The constants A, B , and f_1 are obtainable from the equations given in the literature for most cases of interest. For cases not yet explored mathematically, their determination requires the application of electromagnetic wave theory, a process often difficult and too lengthy to discuss here. However,

* Received by the IRE, October 30, 1959.

TABLE II
VALUES OF CONSTANTS DEPENDENT ON CONFIGURATION AND MODE

MEDIUM	MODE	CUTOFF		A	B
		$f_1 = \alpha f_c$	$\lambda_1 = \lambda_c / \alpha$		
 PAIR OF WIRES	PRINCIPAL	(NOTE 1) 0	∞	$\frac{1}{\sqrt{1-(a/b)^2} \cosh^{-1} b/a}$	0
	 COAXIAL CABLE	PRINCIPAL	0	∞	$\frac{1+a/b}{\text{LOG}_e a/b}$ MIN=3.59, WHEN a/b=3.59
 WAVEGUIDE - RECTANGULAR	TE ₁₀	$\frac{v}{2}$	2	$\frac{a}{b}$	2
	TE _{mn}	$\frac{v}{2} \sqrt{m^2 + n^2 \frac{a^2}{b^2}}$	$\frac{2}{\sqrt{m^2 + n^2 \frac{a^2}{b^2}}}$	$\frac{a}{b} \frac{m^2 + \frac{a}{b} n^2}{m^2 + \frac{a^2}{b^2} n^2} \cdot \frac{2}{S_m S_n}$	$2 \left(\frac{1}{S_m} + \frac{a}{b S_n} \right) - A$
	TM _{mn} (m > 1, n > 1)	$\frac{v}{2} \sqrt{m^2 + n^2 \frac{a^2}{b^2}}$	$\frac{2}{\sqrt{m^2 + n^2 \frac{a^2}{b^2}}}$	$\frac{m^2 + \frac{a^3}{b^3} n^2}{m^2 + \frac{a^2}{b^2} n^2}$	(NOTE: m=0, S _m =2; m≠0, S _m =1 SIMILARLY FOR S _n) 0
 WAVEGUIDE - CIRCULAR	TE _{mn}	$\frac{v}{2\pi} r'_{mn}$	$\frac{2\pi}{r'_{mn}}$	$\frac{m^2}{(r'_{mn})^2 - m^2}$	1
	TM _{mn}	$\frac{v}{2\pi} r_{mn}$	$\frac{2\pi}{r_{mn}}$	1	0

NOTE: $r_{mn} = n^{+h}$ ROOT OF $J_m(r)$; $r'_{mn} = n^{+h}$ ROOT OF $J'_m(r)$

NOTE 1: $v = \text{VELOCITY IN UNBOUNDED DIELECTRIC} = 1/\sqrt{\mu\epsilon} = c/\sqrt{\mu_r\epsilon_r}$

as stated earlier, we have proved the existence of these constants for all cases in the previously defined class. The values of these constants for several common cases are given in Table II.¹

It will be observed that (1) and (2) are analogous to the well-known equation,

$$\alpha = \frac{R}{2R_0} + \frac{GR_0}{2} \quad (5)$$

where R is the effective series ac resistance per unit length, G is the effective shunt conductance per unit length, and R_0 is the real part of the characteristic impedance. Obviously D is dimensionally similar to $GR_0/2$; and since $M\sqrt{f}$ is equal to the surface resistance of the conductor divided by η , the first part of the equation is dimensionally similar to $R/2R_0$.

The discussion above probably contains little that is new to those well versed in electromagnetic theory. However, we believe the engineering usefulness of the equation in the form given, plus the realization of its generality, justifies this communication.

D. K. GANNETT
ZOLTAN SZEKELY
Bell Telephone Labs., Inc.
Murray Hill, N. J.

¹ Some of these values were obtained from equations given in G. C. Southworth, "Principles and Applications of Waveguide Transmission," D. Van Nostrand Co., New York, N. Y., pp. 94-95; 1950.

General Properties of the Propagation Constant of a Nonreciprocal Iterated Circuit*

Complementing an effort to introduce nonreciprocal loss into a microwave iterated circuit, a theoretical determination has been made of the behavior of the propagation constant of a general iterated circuit containing nonreciprocal components. This circuit might find use in a traveling-wave tube or parametric amplifier.

The model examined was an infinitely long chain of identical two-port networks, each specified by the matrix

$$(Z) = \begin{pmatrix} z_{11} & z_{12} \\ z_{21} & z_{22} \end{pmatrix},$$

where $z_{12} \neq z_{21}$ since each network contains nonreciprocal components. Voltages (and currents) to the right and left of each network are assumed to be related by the factor $e^{j\Theta}$ and the problem is to examine the nature of Θ .

The voltages and currents of the system are related by

$$\begin{pmatrix} V_n \\ V_{n+1} \end{pmatrix} = (Z) \begin{pmatrix} I_n \\ -I_{n-1} \end{pmatrix} \quad (1)$$

where n refers to the n th network and $e^{j\Theta} = V_{n+1}/V_n = I_{n+1}/I_n$. Eq. (1) may be expanded and put into the form

$$z_{12}e^{j\Theta} + z_{21}e^{-j\Theta} = z_{11} + z_{22}. \quad (2)$$

Use is made of the following definitions

$$\frac{z_{21}}{z_{12}} = e^{2(jb-\psi)},$$

$$\phi = b + (\text{angle of } z_{12}),$$

$$\Theta = \theta + j\chi,$$

$$x = 1/2 \frac{\text{Im}(z_{11} + z_{22})}{|z_{12}|},$$

$$r = 1/2 \frac{\text{Re}(z_{11} + z_{22})}{|z_{12}|},$$

$$P_c(x) = e^{\psi}(r \cos \phi + x \sin \phi),$$

$$P_s(x) = e^{\psi}(r \sin \phi - x \cos \phi). \quad (3)$$

After a little algebra, (2) may be written

$$\cos(\theta - b) \cosh(\chi - \psi) = P_c(x)$$

$$\sin(\theta - b) \sinh(\chi - \psi) = P_s(x). \quad (4)$$

Finally, conservation of energy requires that

$$r \geq 1/2 |1 + e^{2(j\phi-\psi)}| \geq 0. \quad (5)$$

Although all quantities are basically a function of frequency, it will be convenient to consider x as an independent variable and r as a parameter. Although specific values of x and r do not determine the other quantities uniquely, they do determine upper and lower bounds on the other quantities. The cases of $r=0$ and $r>0$ will now be treated.

(1) $r=0$ (lossless case). From (5), $\psi=0$, $P_c(x)=x$, and $P_s(x)=0$, so that (4) becomes

$$\cos(\theta - b) \cosh \chi = x$$

$$\sin(\theta - b) \sinh \chi = 0. \quad (6)$$

Eq. (6) has the simultaneous solution

$$\left. \begin{aligned} \cos(\theta - b) &= x \\ \chi &= 0 \end{aligned} \right\} -1 \leq x \leq 1,$$

$$\left. \begin{aligned} \theta - b &= m\pi \\ \cosh \chi &= (-1)^m x \end{aligned} \right\} |x| \geq 1.$$

χ and $\theta - b$ are plotted vs x as the solid curves in Figs. 1 and 2 where it is understood that

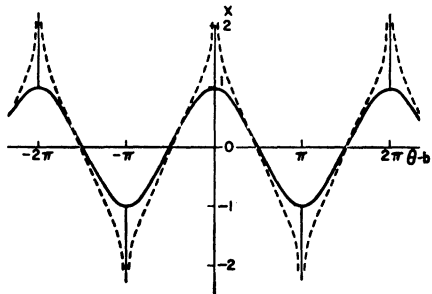


Fig. 1.

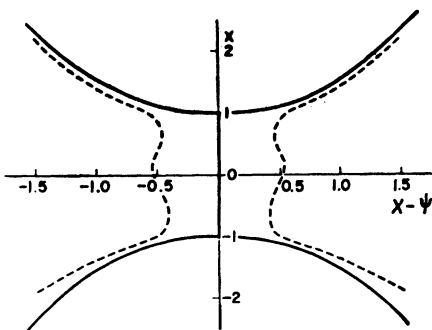


Fig. 2.

$\psi = 0$. The structure has a pass band from $-1 \leq x \leq 1$. Within this range, the loss parameter χ is zero and the phase parameter θ varies from $m\pi + b$ to $(m \pm 1)\pi + b$. For x above 1 and below -1 , the loss parameter is high and the phase parameter is $m\pi + b$. The significant difference between the nonreciprocal and reciprocal cases is that in the latter x is an even function of θ , i.e., $b = 0$. In the former case, this is no longer true. At $\theta = 2\pi m$, x is not 1 but $\cos b$. Thus, for a nonreciprocal circuit, the propagation constants of the space harmonics will depend on the direction of propagation. A plot of x vs θ would look like Fig. 1 except that the curve shown in Fig. 1 would be shifted to the left or right of the ordinate by an amount b . If b is not a constant but a function of x , the situation is further complicated.

2) $r > 0$ (lossy case). For $r > 0$, (5) indicates that it is only possible to determine ϕ and ψ to within a band of values whose upper and lower limits may be calculated. Thus, for specific values of r and x , P_c and P_s may be determined to within a band whose upper and lower limits may be calculated. Nevertheless, from this information, it is possible to predict the general behavior of the loss and phase parameters. Typical plots of these parameters vs x are shown as the dotted curves in Figs. 1 and 2.

As an aid in determining these plots, we write (4) in the form

$$\sin^2(\theta - b) = P_c^2(x) \tan^2(\theta - b) - P_s^2(x),$$

$$\sinh^2(\chi - \psi)$$

$$= P_c^2(x) \tanh^2(\chi - \psi) + P_s^2(x) \quad (7)$$

and note the intersection of the left and right hand sides of each equation as P_c and

P_s are given their extreme values holding r fixed and varying x .

The behavior of χ and θ for $r > 0$ is more or less an expected extension of the $r = 0$ case except that now the loss parameter depends on the direction of propagation since $\psi \neq 0$. A plot of χ vs x would be the plot of Fig. 2 shifted to the left or right of the ordinate by an amount ψ . If ψ is a function of x , the situation is further complicated.

Two points of practical importance should be noted about an iterated nonreciprocal circuit used as a traveling-wave tube circuit. First, in a traveling-wave tube, $\theta = \beta L$ where L is the periodic length. In order to get interaction with the electron beam over a maximum of the pass band (from $x = -1$ to $+1$), at midband (frequency corresponding to $x = 0$) β must be approximately equal to the plasma slow-wave propagation constant and $\theta = \theta_{x=0}$. For the reciprocal case, $\theta_{x=0}$ is very close to an odd multiple of $\pi/2$ so that L is determined. In the nonreciprocal case, $\theta_{x=0} = (\text{odd multiple of } \pi/2) + b$ and theoretically may be any angle. Thus, L is not restricted and may be chosen so as to optimize some parameter such as interaction impedance.

Secondly, it can be true that the addition of loss broadens the band of circuit-wave interaction with the electron beam (see Fig. 1, dotted curves). However, the attendant forward-wave loss negates the desirability of doing this. However, in a nonreciprocal circuit, it is theoretically possible to introduce ψ in such a way that the forward loss is small. At the same time, the backward loss increases, which is usually a desirable circuit property.

The author wishes to acknowledge the valuable aid of S. Sensiper of Hughes Aircraft Co. who suggested the problem and who provided subsequent stimulating discussions.

R. N. CARLILE
Dept of Elec. Engrg.
University of California
Berkeley, Calif.
Formerly at Hughes Aircraft Co.
Culver City, Calif.

Parametric Amplifier Antenna*

A number of circuit configurations have been reported¹ for employing voltage variable capacitors as the active element in a parametric amplifier. One form, described by Harris² and others, utilizes a coaxial distributed structure to provide, at the same time, appropriate resonant conditions for both the signal and the so-called idler frequency components. In this mode of operation the input signal and the output are at the same frequency f_s . The pumping energy source may be at $2f_s, 4f_s, \dots$ etc., while the idler will have a corresponding value of f_s ,

* Received by the IRE, October 29, 1959. The work described has been carried out under the sponsorship of the Electronics Research Directorate, Air Force Cambridge Res. Center.

¹ A. Uhlir, Jr., "The potential of semiconductor diodes in high frequency communications," Proc. IRE, vol. 46, pp. 1099-1115; June, 1958.

² B. Salzberg and W. E. Sard, "A low-noise wide-band reactance amplifier," Proc. IRE, vol. 46, p. 1303; June, 1958.

³ F. S. Harris, "The parametric amplifier," CQ, vol. 14, November, 1958.

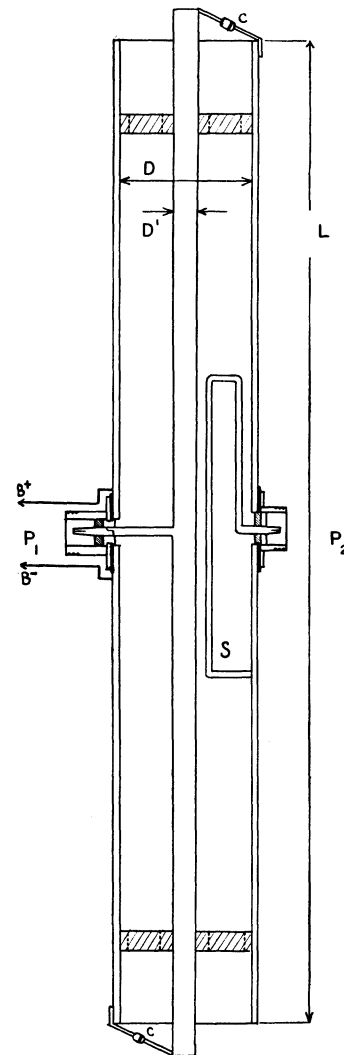


Fig. 1—Cross-sectional view of parametric amplifier antenna or "parant."

$3f_s, \dots$. A number of advantages can be derived by realizing this circuit in a balanced form and incorporating the resulting structure inside of a half wave dipole as shown in Fig. 1. The amplifier consists of the outer cylinder of length L which serves as an antenna, and an inner coaxial conductor, diameter D' , supported at the center by an RF connector and low loss dielectric spacers as shown. Each end of the center conductor is connected to the corresponding end of the antenna through parametric diodes (HPA 2800) at C and C' . The antenna is split at the mid-point to provide dc isolation for the diode bias paths. A thin dielectric layer between the dipole sections and the central supporting sleeve serves as an RF bypass path for antenna currents. The pumping signal is applied to both diodes in phase through the inner conductor at P_1 . With the center conductor at dc ground, either through the generator or a suitable transmission line stub, diode bias voltages are applied at $B+$ and $B-$. In operation the interior coaxial region serves as a resonant storage volume for both the signal and idler components. The output is taken at P_2 from loop S through a suitable network which passes f_s while rejecting f_i .

Fig. 2 shows the inner construction of a unit designed for use at 220 mc. Fig. 3 is the assembled antenna-amplifier dipole. It is necessary that the physical length of the

antenna cylinder be adjusted for the desired center operating frequency while at the same time the coaxial system is resonant at f_0 and an odd multiple of f_0 . Since the free resonant length of an antenna is significantly less than $\lambda/2$ the interior system would appear to have less than its requisite electrical length. It has been found, however, that with the antenna units investigated to date an adjustment of fringing and diode capacitance has been sufficient to achieve the simultaneous resonance conditions without the use of an internal dielectric septum. Antenna-amplifier gain, relative to a passive dipole of the same length and diameter and measured as a function of frequency, is shown in Fig. 4.

In addition to the advantage of a potentially low noise figure such as is common to reactive parametric amplifiers, this arrangement provides a low impedance output at a coaxial connection in the neutral plane of the antenna. Complications in construction arising from the use of a split outer conductor can be avoided by separating the inner conductor into two sections at the

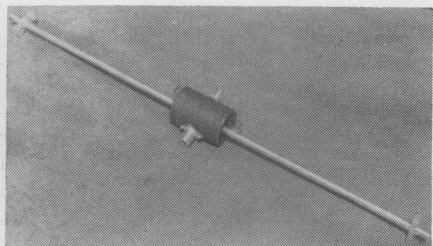


Fig. 2—Antenna center conductor showing output loop and coaxial connectors.

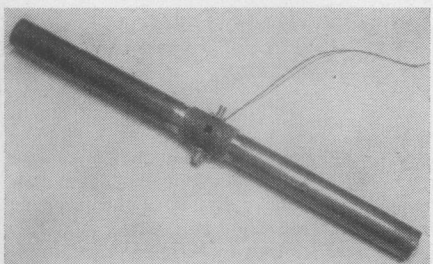


Fig. 3—Assembled antenna amplifier dipole.

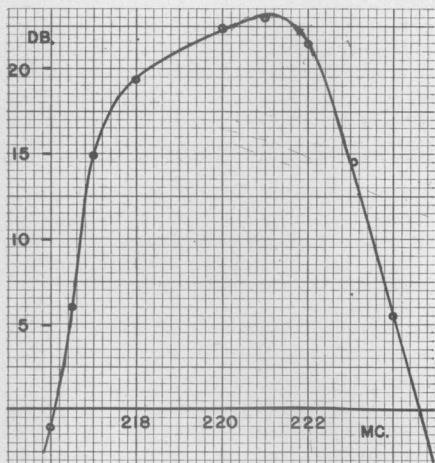


Fig. 4—Antenna amplifier gain relative to passive dipole having the same length and diameter. Pumping source frequency and dc bias adjusted at each point for maximum gain.

center and applying the pumping and bias voltages through a twin coaxial connector instead of the type N as used in this version.

ALBERT D. FROST
Antenna Systems Lab.
Dept. of Elec. Engrg.
University of New Hampshire
Durham, N. H.

Superdirectivity*

Kock¹ in his interesting paper on "Related Experiments with Sound Waves and Electromagnetic Waves" credits Schelkunoff² with the first discussion of superdirectivity in aerial arrays. Though Dr. Schelkunoff's paper is of basic importance in this field, investigation of the phenomenon commenced much earlier. The first demonstration of the possibility of superdirectivity that we know of was published in 1922 by C. W. Oseen.³ Reference to four other papers prior to that of Schelkunoff was given by us in a previous paper.⁴ In the bibliography appended to that paper, we listed all the work on superdirectivity then known to us; the quite impressive total of twenty-eight items resulted. In view of the continued interest in this subject it may be of value to bring this listing up to date, as attempted in the bibliography below. For the Goward reference [1] we are indebted to Mr. J. D. Lawson of the Atomic Energy Research Establishment at Harwell.

A. BLOCH,
R. G. MEDHURST,
S. D. POOL
Research Laboratories,
The General Electric Co., Ltd.
Wembley, England.

Author's Comment:⁵

I feel that Oseen³ discussed the possibility of superdirectivity, whereas Schelkunoff² and Franz [28] demonstrated a feasible method of approach to its realization. Schelkunoff U. S. Pat. No. 2,286,839 on this subject was applied for on December 20, 1939; it was issued on June 16, 1942. I am indebted to Dr. Franz for the receipt of reprints of two papers of his [28, 30] which appeared during the war and which I failed to reference. The second [30] refers to still another author on superdirectivity: A. Fradin, *J. O. A. Ph.*, Leningrad, Russia, vol. 9, p. 1161; 1939.

WINSTON E. KOCK
Research Laboratories Div.
Bendix Aviation Corp.
Detroit, Mich.

* Received by the IRE, November 4, 1959.

¹ W. E. Kock, "Related experiments with sound waves and electromagnetic waves," *Proc. IRE*, vol. 47, pp. 1192-1201; July, 1959.

² S. A. Schelkunoff, "A mathematical theory of linear arrays," *Bell Sys. Tech. J.*, vol. 22, pp. 80-107; January, 1943.

³ C. W. Oseen, "Die Einsteinsche, Nadelstichstrahlung und die Maxwell'schen Gleichungen," *Ann. der Phys.*, vol. 69, pp. 202-204; 1922.

⁴ A. Bloch, R. G. Medhurst, S. D. Pool, "A new approach to the design of super-directive aerial arrays," *Proc. IEE (London)*, pt. III, vol. 100, pp. 303-314; September, 1953.

⁵ Received by the IRE, November 25, 1959.

BIBLIOGRAPHY

- [1] F. K. Goward, "An improvement in end-fire arrays," *Proc. IEE, (London)*, vol. 94, pp. 415-418; November, 1947.
- [2] R. L. Pritchard and M. D. Rosenberg, "Optimum directivity patterns for linear arrays," *J. Acoust. Soc. Amer.*, vol. 20, pp. 594-595; July, 1948.
- [3] H. L. Knudsen, "Superforstærkning hos antenner," *Elektrotek Tidsskr.*, vol. 64, pp. 213-221; June 5, 1951. (In Danish)
- [4] G. Sinclair and F. V. Cairns, "Optimum patterns for arrays of non-isotropic sources," *IRE TRANS. ON ANTENNAS AND PROPAGATION*, vol. AP-1, pp. 50-59; February, 1952.
- [5] A. S. Dunbar, "On the theory of antenna beam shaping," *J. Appl. Phys.*, vol. 23, pp. 847-853; August, 1952.
- [6] L. L. Bailin and M. J. Ehrlich, "Factors affecting the performance of linear arrays," *Proc. IRE*, vol. 41, pp. 235-241; February, 1953.
- [7] R. H. DuHamel, "Optimum patterns for endfire arrays," *Proc. IRE*, vol. 41, pp. 652-659; May, 1953.
- [8] A. A. Pistolokors, "Use of Mathieu functions for computing field distribution in an antenna to obtain a given directional diagram," *Dokl. Akad. Nauk SSSR*, vol. 89, no. 5, pp. 849-852; April 11, 1953; *Natl. Sci. Foundation transl. NSF-tr-113*.
- [9] L. D. Bakhrakh, "A solution of the integral equation for a linear antenna," *Dokl. Akad. Nauk SSSR*, vol. 92, no. 4, pp. 755-758, October 1, 1953; *Natl. Sci. Foundation transl. NSF-tr-211*, February, 1954.
- [10] R. L. Pritchard, "Optimum directivity patterns for linear point arrays," *J. Acoust. Soc. Amer.*, vol. 25, pp. 879-891; September, 1953.
- [11] ———, "Maximum directivity index of a linear point array," *J. Acoust. Soc. Amer.*, vol. 26, pp. 1034-1039; November, 1954.
- [12] T. T. Taylor, "Design of line-sources for narrow beamwidth and low side-lobes," *IRE TRANS. ON ANTENNAS AND PROPAGATION*, vol. AP-3, pp. 16-28; January, 1955.
- [13] R. L. Pritchard, "Discussion on optimum patterns for endfire arrays," *IRE TRANS. ON ANTENNAS AND PROPAGATION*, vol. AP-3, pp. 40-43; January, 1955.
- [14] E. N. Gilbert and S. P. Morgan, "Optimum design of directive antenna arrays subject to random variations," *Bell Sys. Tech. J.*, vol. 34, pp. 637-663; May, 1955.
- [15] R. Kovács and L. Solymár, "Theory of aperture aerials based on the properties of entire functions of the exponential type," *Acta Phys. Acad. Sci. Hung.*, vol. 6, no. 2, pp. 161-184; 1956.
- [16] M. Uzsoky and L. Solymár, "Theory of super-directive linear arrays," *Acta Phys. Acad. Sci. Hung.*, vol. 6, no. 2, pp. 185-205; 1956.
- [17] G. T. di Francia, "Directivity, super-gain and information," *IRE TRANS. ON ANTENNAS AND PROPAGATION*, vol. AP-4, pp. 473-479; July, 1956.
- [18] A. Bloch, "N-terminal networks: some theorems with applications to the directive properties of aerial arrays," *Wireless Engr.*, vol. 33, pp. 295-300; December, 1956.
- [19] V. L. Pokrovskii, "On the theory of optimal linear antennas," *Radio Engrg. and Electronics*, vol. 2, no. 12, p. 123; 1957.
- [20] D. G. Tucker, "Signal/noise performance of super-directive arrays," *Acustica*, vol. 8, no. 2, pp. 112-116; 1958.
- [21] L. Solymár, "A reactance theorem for antennas," *Proc. IRE*, vol. 46, p. 779; April, 1958.
- [22] ———, "Maximum gain of a line source antenna if the distribution function is a finite Fourier series," *IRE TRANS. ON ANTENNAS AND PROPAGATION*, vol. AP-6, pp. 215-219; July, 1958.
- [23] R. F. Harrington, "On the gain and beamwidth of directional antennas," *IRE TRANS. ON ANTENNAS AND PROPAGATION*, vol. AP-6, pp. 219-225; July, 1958.
- [24] G. Broussard, "Contribution à l'étude théorique rayonnement," in "Comme. Prés. au Congrès International Circuits et Antennes Hyperfréquences," 1957, vol. 1, pp. 58-62, suppl. to *L'Onde Elec.*; August, 1958.
- [25] N. F. Barber, "Design of 'optimum' arrays for direction-finding," *Elec. and Radio Engr.*, vol. 36, pp. 222-232; June, 1959.
- [26] J. D. Lawson, "Electromagnetic wave problems," *Elec. and Radio Engr.*, vol. 36, pp. 332-338; September, 1959.
- [27] R. F. Kyle, "Super-gain aerial beam," *Elec. and Radio Engr.*, vol. 36, pp. 338-340; September, 1959.
- [28] K. Franz, "Die Verbesserung des Uebertragungs-wirkungsgrades durch Richtantennen," *Telefunken Mitteilungen*, vol. 21, pp. 3-8; 1940.
- [29] J. C. Simon, G. Broussard, and E. Spitz, "Sur la superdirectivité d'une antenne à rayonnement transversal," *Comptes Rend. Acad. Sci.*, vol. 248, pp. 2309-2311; April, 1959.
- [30] ———, "Bemerkungen über die Absorptionsfläche von Richtantennen," *Hochfr. u. Elek-tronik*, vol. 61, pp. 51-53; 1943.
- [31] L. D. Bakhrakh, "The maximal directivity coefficient of linear and plane aerials," *Dokl. Akad. Nauk SSSR*, vol. 95, pp. 45-48; March 1, 1954.

Parallel Field Excitation*

AT-cut circular quartz plates or lenses are used for the control of precision oscillators in the range of 500 to 2500 kc.

The major requirements are: high *Q*, freedom of unwanted responses, and a good frequency-temperature behaviour.

As the inductance of these crystals is low, it is necessary to reduce by all means the resistance of the crystals in order to obtain high *Q* values. Good crystals, however, have a very low resistance of about one to five ohms. This complicates the design of the oscillator from the point of view of impedance matching.

As a result of recent work performed at the Paris Observatory, as well as at Oscilloquartz Dept. of Ebauches S.A. at Neuchatel, Switzerland, the electric parameters of the crystals were altered by application of an electric field parallel to the major surfaces of the crystal; this is instead of having it normal to the surfaces, as it is usually done for the excitation of thickness-shear vibrations.

There are two main points to consider when the parallel field method is applied:

- 1) Inductance and resistance are rising, but the former rises quicker than the latter; thus the *Q* value increases.
- 2) The resistance of unwanted responses is highly increased, especially that of unwanted face shear modes.

For one-mc fundamental-mode plated lenses of about 27-mm diameter, *Q* values between 6 and 8 · 10⁶ have been obtained. For 0.5-mc fundamental-mode plated lenses of about 38-mm diameter, the *Q* is approximately 8 to 10 · 10⁶. For both types, the resistance has values between 45 and 80 ohms, and the inductance is approximately 50 times higher than the inductance of crystals excited by a field normal to the surfaces.

Much higher *Q*'s are obtained with *non-plated* crystals excited by the parallel field. Depending upon the choice of the geometry of the electrodes and of the air gap, the *Q*'s of 0.5- and 1-mc lenses are approximately 20 · 10⁶.

All the measurements mentioned above have been made at room temperature.

V. IANOUCHEVSKY
Observatoire de Paris
Paris, France

BIBLIOGRAPHY

R. Bechman, "Filterquarze im Bereich 7 bis 30 MHz," Arch. Elek. Übertragung, vol. 13, pp. 90-93; 1959.
R. Bechmann, "Improved High-Precision Quartz Oscillators," Proc. IRE, vol. 48, pp. 367-368; March, 1960.

* Received by the IRE, November 6, 1959.

Theoretical Hysteresis Loops of Thin Magnetic Films*

The theoretical static behavior of single domain thin magnetic films can be determined on the basis of a few hypotheses:

- 1) The magnetization vector has a constant amplitude *M_s*.
- 2) It lies in the plane of the film.
- 3) The total energy per unit volume of the film is

$$E = K \sin^2 \theta - HM_s \cos(\phi - \theta) \quad (1)$$

The first term in (1) is the uniaxial anisotropy energy, where *K* is the anisotropy constant and θ the angle between the magnetization vector and the preferred direction of magnetization (easy direction). The second term is the energy of magnetization in the applied field of amplitude *H* and of direction ϕ .

Magnetization curves obtained from (1) are analyzed as a function of ϕ by Stoner and Wohlfarth¹ and for crossed fields by Smith.² Chu and Singer³ give a graphical method, based on these energy considerations, for the determination of theoretical hysteresis loops. This communication gives a simple analytical method as well as a graphical construction more accurate and easier than the first method, which is sometimes difficult because of the flatness of the energy minimum. As is known, the magnetization assumes the direction in which the total energy *E* is a minimum.

$$\frac{\partial E}{\partial \theta} = 0; \quad \frac{\partial^2 E}{\partial \theta^2} > 0. \quad (2)$$

Two stable orientations exist for certain values of the field. By a continuous variation of the field vector, a jump occurs when

¹ E. C. Stoner and E. P. Wohlfarth, "A mechanism of magnetic hysteresis in heterogeneous alloys," *Phil. Trans. Roy. Soc., A*, vol. 240, pp. 599-642; 1948.
² D. O. Smith, "Static and dynamic behaviour of thin permalloy films," *J. Appl. Phys.*, vol. 29, pp. 264-273; March, 1958.
³ K. Chu and J. R. Singer, "Thin film magnetization analysis," *Proc. IRE*, vol. 47, pp. 1237-1244; July, 1959.

the present minimum disappears; this case is realized when

$$\frac{\partial^2 E}{\partial \theta^2} = 0. \quad (3)$$

An analytical expression for the theoretical hysteresis loop, given by (1) and (2), is easy to obtain. The easy and hard directions are called *x* and *y*. The projections *H_x* and *H_y* of the field and the projections *M_x* and *M_y* of the magnetization are considered. *M_x* and *M_y* are related to the angle θ by

$$M_x = M_s \cos \theta; \quad M_y = M_s \sin \theta. \quad (4)$$

Reduced variables can be introduced in order to get dimensionless equations:

$$h_x = \frac{H_x M_s}{2K}; \quad h_y = \frac{H_y M_s}{2K};$$

$$m_x = \frac{M_x}{M_s}; \quad m_y = \frac{M_y}{M_s}. \quad (5)$$

Combination of (1), (2), (4) and (5) gives the system:

$$m_x^2 + m_y^2 = 1$$

$$\frac{h_x}{m_x} - \frac{h_y}{m_y} = -1. \quad (6)$$

The simplest way to compute hysteresis loops in the easy and hard directions, by means of these equations, is to consider *m_x* or *m_y* as the independent variable and *h_y* or *h_x* as a parameter, and then to compute *h_x* or *h_y*. The four main cases are shown in Fig. 1(a) below, and Fig. 1(b), next page. The jumps in the first two curves occur when $\partial h_x / \partial m_x = 0$ which, combined with (6), gives

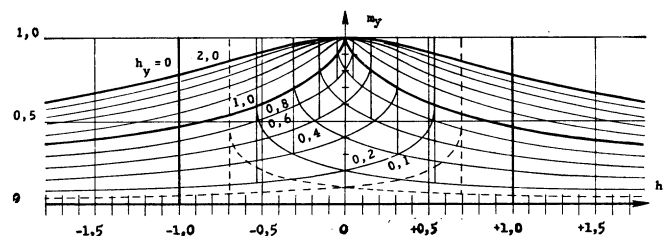
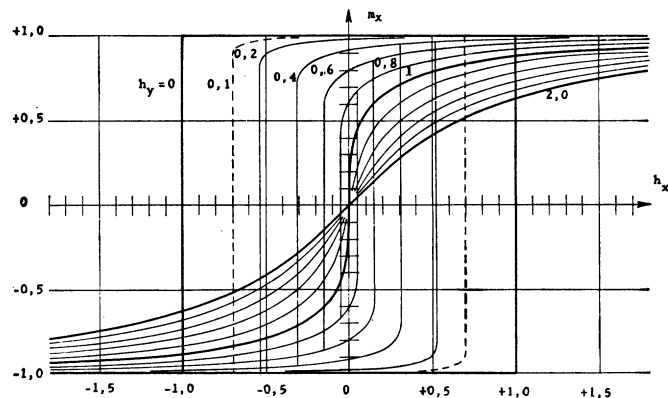


Fig. 1(a)

* Received by the IRE, November 2, 1959.

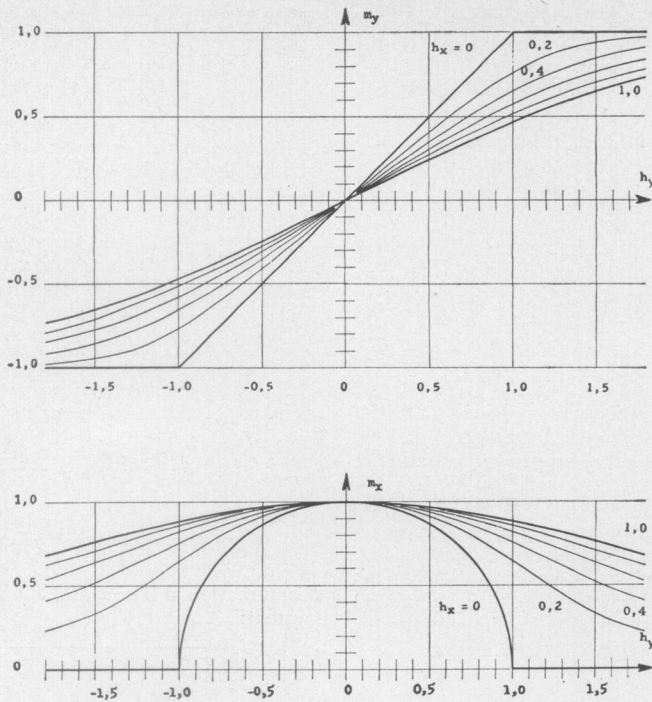


Fig. 1(b)

Fig. 1—Magnetization projection m_x and m_y . (a) As a function of the field h_x in the easy direction and with the field h_y in the hard direction as parameter; (b) as a function of the field h_y in the hard direction and with the field h_x in the easy direction as parameter.

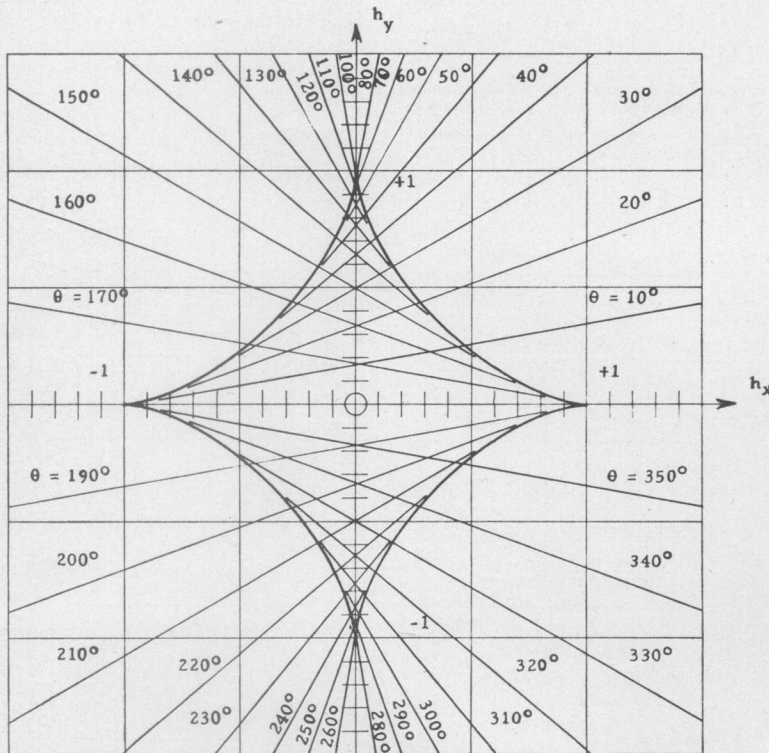


Fig. 2—Critical curve and geometrical construction of the magnetization direction θ .

the relation

$$h_x^{2/3} + h_y^{2/3} = 1. \quad (7)$$

This equation represents the critical curve. The magnetization just before a jump is

$$m_x = h_x^{1/3}; \quad m_y = h_y^{1/3}. \quad (8)$$

In the easy direction, the curves are reversible when $h_y \geq 1$. The initial susceptibility in the reduced curves is then

$$\frac{\partial m_x}{\partial h_x} \Big|_{h_x=0} = \frac{1}{h_y - 1}$$

In the hard direction, the curves are always reversible, and the initial susceptibility is

$$\frac{\partial m_y}{\partial h_y} \Big|_{h_y=0} = \frac{1}{h_x + 1}$$

An essential property of (6) is the linear dependence of h_x and h_y for a given value of m_x , m_y or of the direction θ of the magnetization vector. Furthermore, it can be shown⁴ that all the straight lines in the (h_x, h_y) plane are tangential to the critical curve (7). This property can be used for the graphical determination of hysteresis loops under various conditions (Fig. 2), as first proposed by Slonczewski.⁵ The straight line going through the point (h_x, h_y) and tangential to the critical curve forms, with the x axis, an angle θ equal to the angle formed by the magnetization vector with the easy direction.

Experimental curves agree very well with the theoretical curves obtained under the simplified initial hypotheses, provided single domain structure and rotational processes only take place. This is the case for the reversible curves shown in Fig. 3.

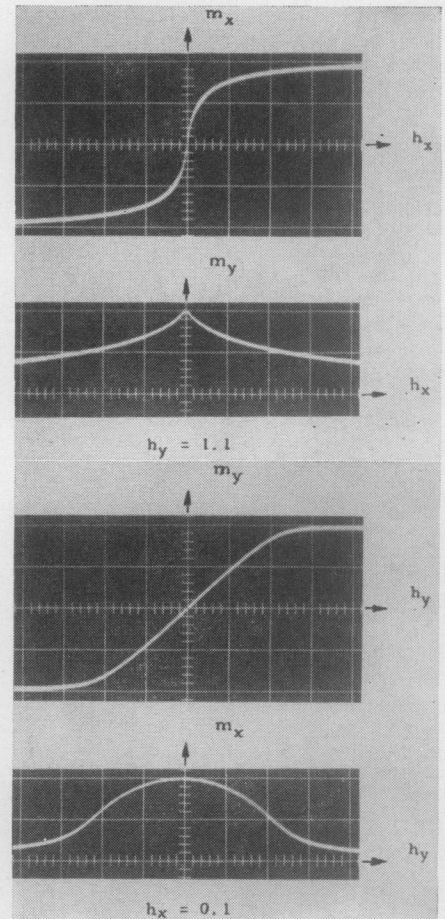


Fig. 3—Experimental M-H loops of a Ni-Fe film of about 80-20 composition show rotational and reversible behavior at low frequency (500 cps).

H. J. OGUEY
Res. Lab., IBM Corp.
Zurich, Switzerland

⁴ P. Franklin, "Advanced Calculus," McGraw Hill Book Co., Inc., New York, N. Y., p. 343: 1944.
⁵ J. C. Slonczewski, "Theory of magnetic hysteresis in films and its application to computers," IBM Rept. No. RM 003.111.224. October 1 1956 (unpublished).

Narrow-Band Filtering of Random Signals*

The misconception that the output of a narrow-band filter is more nearly Gaussian than some corresponding non-Gaussian random input appears to be widespread. The incorrectness of this concept is demonstrated by the following examples.

First, consider the random process consisting of the pure cisoids,

$$x(t) = e^{2\pi j(f t + \phi)}, \quad -\infty < t < \infty,$$

where the frequency f is a random variable with arbitrarily given probability distribution,

$$\Pr\{f \leq \lambda\} = F(\lambda), \quad -\infty < \lambda < \infty,$$

and the random phase ϕ is uniformly distributed on the unit interval. The process thus defined¹ is stationary in the wide sense, with autocovariance easily seen to be

$$\langle x(t_1) \overline{x(t_2)} \rangle = \int_{-\infty}^{\infty} e^{2\pi j \lambda (t_1 - t_2)} dF(\lambda). \quad (1)$$

[Note that any (unit power) power spectrum may be thus realized.] If this process is applied as input to a filter with transfer function

$$Y(2\pi j f) = \begin{cases} 1 & f' < f \leq f'' \\ 0 & \text{otherwise,} \end{cases} \quad (2)$$

then the output, renormalized to unit power, has at any fixed time the form,

$$\begin{aligned} &\Delta^{-1/2} e^{2\pi j \theta} \text{ with probability } \Delta, \\ &0 \text{ with probability } 1 - \Delta, \end{aligned}$$

where $\Delta = F(f'') - F(f')$, and where θ is a random variable uniformly distributed on the unit interval. This distribution of the output does not approximate the (complex) unit normal distribution in any reasonable sense as $f'' - f' \rightarrow 0$. The analogous real process and filter also give rise to a non-Gaussian output distribution.

A more striking example is provided by

$$x(t) = n^{-1/2} \sum_{\nu=1}^n e^{2\pi j(f_{\nu} t + \phi_{\nu})}, \quad -\infty < t < \infty, \quad (3)$$

where f_{ν} , ϕ_{ν} , $\nu = 1, \dots, n$ are mutually independent random frequencies and phases, respectively, each distributed as in the example above. The autocovariance of process (3) is given by (1), as before. If n is large, then the distribution of $x(t)$ of (3) at any fixed time will be nearly Gaussian, by the central limit theorem. If now f' and f'' are chosen so that $n\Delta$ is moderately small (say $n\Delta < 0.25$) then the output of filter (2) will have at any fixed time the form (again, renormalized to unit power)

$$\begin{aligned} &0 \text{ with probability } 1 - n\Delta + O((n\Delta)^2) \\ &(n\Delta)^{-1/2} e^{2\pi j \theta} \text{ with probability } n\Delta + O((n\Delta)^2) \\ &(\text{other}) \text{ with probability } O((n\Delta)^2), \end{aligned}$$

with Δ and θ as before. Thus a random signal whose distribution at any fixed time is nearly Gaussian is converted by narrow-band filtering to one whose variables are much less Gaussian.

It may be argued that the processes described above are not ergodic and the author is willing to admit the possibility that narrow-band filtering of a non-Gaussian stationary (wide sense) process which is ergodic in the wide sense² might give a process whose variables are individually more nearly Gaussian. However, the above examples indicate that a proof will have to be more delicate than the heuristic arguments usually given. (In these arguments, small correlation is confused with small stochastic dependence.)

S. P. LLOYD
Bell Telephone Labs.
Murray Hill, N. J.

² By this we mean a process whose sample function autocorrelations (time average) are equal to the process autocovariance (statistical average) with probability 1; the definition of Doob is different. See J. L. Doob, *op. cit.*, pp. 461-464, 493-497.

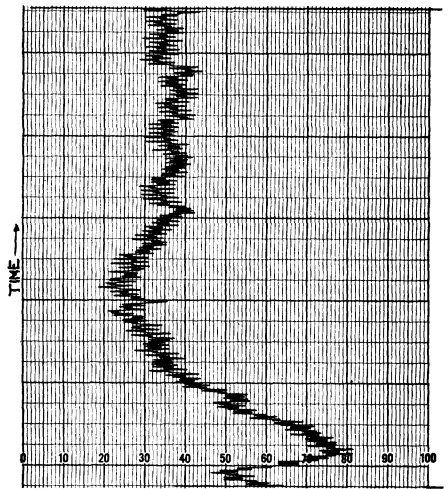


Fig. 1(a)

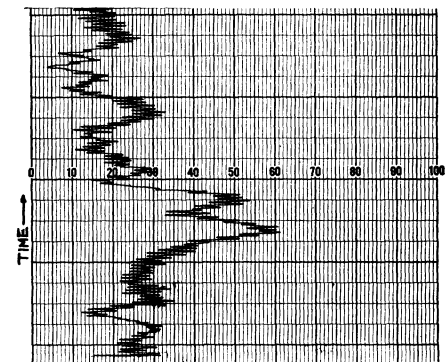


Fig. 1(b)

Rapid Periodic Fading of Medium Wave Signals*

The occurrence of a peculiar type of rapid fading, called "flutter phenomenon," in broadcast signals have been reported by Subba Rao and Somayajulu.¹ They observed this type of fading regularly on the 41-m and 61-m bands and occasionally on the 19-m band, but never on the medium wave band. Recently, Yeh and Villard² reported the occurrence of a more rapid fading of signals in the 41-m band propagating over long paths crossing the magnetic equator.

Using a superheterodyne broadcast receiver, the AVC system of which was disconnected, and a recording millivoltmeter, it has been possible to record the same type of rapid fading of signals on the medium wave as well as short wave bands. A few typical records are reproduced here. The particulars of these records are as follows: Fig. 1(a) shows fading of transmission in the 19-m band from Karachi, received at 1935 hours Indian Standard Time (IST) on March 3, 1959. Fig. 1(b) shows the same in the 61-m band from Madras, received at 1845 hours IST the same day. Fig. 2(a) is a record of such fading of signals at 280.4-m received from Delhi at 2027 hours IST, also the same day. Fig. 2(b) represents another such record of the 280.4-mc signals obtained at 1912 hours IST on March 16, 1959 and

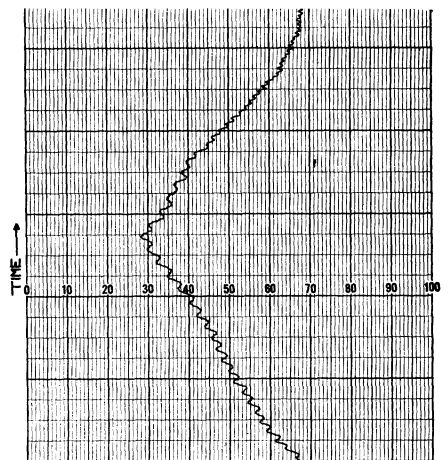


Fig. 2(a)

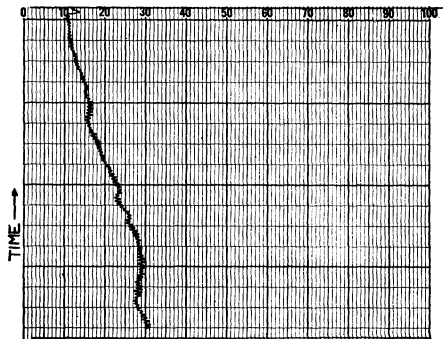


Fig. 2(b)

* Received by the IRE, October 22, 1959.

¹ N. S. Subba Rao and V. V. Somayajulu, "A peculiar type of rapid fading in radio reception," *Nature*, vol. 163, p. 442; March, 1949.

² K. C. Yeh and O. G. Villard, Jr., "A new type of fading observable on high-frequency radio transmissions propagated over paths crossing the magnetic equator," *Proc. IRE*, vol. 46, pp. 1968-1970; December, 1958.

* Received by the IRE, October 22, 1959.
¹ J. L. Doob, "Stochastic Processes," John Wiley and Sons, Inc., New York, N. Y., p. 525; 1953. It is to be emphasized that each sample function of the process is a pure cisoid, of fixed frequency and phase, extending indefinitely in time. The random element is the choice of frequency and phase.

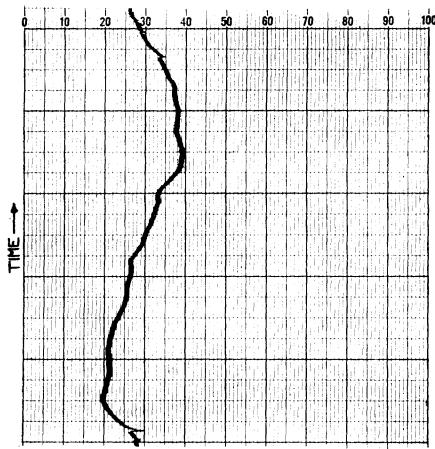


Fig. 2(c)

Fig. 2(c) shows a more rapid fading of the same signals at 1850 hours IST on March 12, 1959. On the time axis, four large divisions represent one minute.

It may be noted that the rate of fading of the medium wave signals is of the same order as that of the short wave signals, namely, about 1.5 to 3 cps. No known mode of propagation can account for such a rate of fading at this wavelength. Further records are being made.

The gift of a Varian type G-10 graphic recorder from the U. S. Government under the India Wheat Loan Educational Exchange Scheme is gratefully acknowledged.

HARIHAR MISRA
Physics Department
Ravenshaw College
Cuttack 3, India

Report on the AGU Study of the Metric System in the United States

The American Geophysical Union's Special Committee for the Study of the Metric System in the United States has noted the recent publication of our "Letter to the Editor" and its accompanying Questionnaire in the PROCEEDINGS.¹

We wish to express our sincere appreciation for the courtesy of the IRE in presenting this matter to its readers. We wish also to thank your members who aided the Committee by a generous response of completed questionnaires. Many of the replies included letters containing helpful suggestions and offering financial assistance if requested.

Those readers who have access to the September, 1959, *Transactions of the American Geophysical Union* will find there a full report of the Committee, together with an analysis of the replies to the Questionnaire received up to July. At this date, three

months later, 1080 have been analyzed. The scientific and engineering field was rather well covered by publication last spring of the Letter or Questionnaire, or both, in eight of the leading journals and magazines of the United States. Briefly, to the most significant question as to whether it would be desirable to replace the English System with the Metric as the "only official system" of weights and measures in the United States, ninety per cent have replied in the affirmative. The average suggested period of transition was about 22 years; this indicates agreement with the Committee on the necessity for a long transition period to avoid economic dislocation through education in the schools, through a normal retirement of presently active older personnel, and through the normal obsolescence of existing equipment.

The Congress of the United States, for the first time in nearly thirty years, is faced with a decision on metric legislation, recently introduced in both Houses. House Bill, HR7401, May, 1959, by Mr. Brooks of Louisiana, and Senate Bill, S2420, July, 1959, by Mr. Neuberger, both call for a feasibility study of the problem by an appropriate Government agency, with fund authorization. A third action of interest is the introduction in July, 1959, by Representative Fulton, of House Concurrent Resolution 364 which would place the Congress on record in favor of the Metric System.

It is apparent that the United States must soon decide whether to change over gradually, during the next generation, to a far simpler and more logical system of weights and measures, or to continue to live in comparative isolation with the remaining ten per cent of the world's population not yet under the Metric System.

FLOYD W. HOUGH
Chairman, Committee for the
Study of the Metric System
in the United States,
American Geophysical Union
1515 Massachusetts Ave., N. W.
Washington 5, D. C.

Noise Spectrum of Phase-Locked Oscillators*

The fundamental parameter that best describes a phase-locked klystron is the noise spectrum of the oscillator in the phase-locked condition.¹ Some time ago a program for studying the sources of noise in phase-locked oscillators was established in the Microwave Spectroscopy Laboratory of the Research Laboratory of Electronics, Massachusetts Institute of Technology. The fol-

lowing remarks are a summary of the results of this project at its termination.

Since the first demonstration² of the simple utility of phase-locking klystron techniques in the microwave region, there has been considerable concern about the purity and validity of the resulting spectrum. Sources of noise, either amplitude-modulation noise or phase-modulation noise, can arise at many points in the servo-control loop. The importance of the various sources of noise is most convincingly demonstrated by experimental measurement. For this reason, a test facility consisting of two Felch oscillators,³ at 1 mc and 5 mc, was built; active tube multipliers, multiplying to 300 mc and 700 mc, were constructed; and electronic phase-locking equipment for K-band and X-band klystrons was assembled or constructed. The final system is shown in the block diagram of Fig. 1. It consists essentially of a silicon-diode harmonic generator, balanced mixer, 455-kc IF amplifier, phase demodulator, dc amplifier, and phase-correcting network to the klystron repeller. Previous phase-stabilization circuits measured in this laboratory have indicated a carrier noise level of approximately 60 db/cps.⁴ It was our intention to use the measurements for comparing the noise amplitude as a function of the multiplication ratio and as a function of the low-frequency crystal-reference oscillator frequency.

Two klystrons were stabilized in this fashion and were beaten against each other in a superheterodyne receiver; the resulting beat note (arising from a small difference in the fundamental crystal-oscillator frequencies) could be displayed on an oscilloscope and the carrier-to-noise ratio could be analyzed with a General Radio harmonic distortion analyzer.

Unfortunately, when the system reached satisfactory operating condition, it was found that even with a frequency multiplication of 10,000 from a low-level Felch crystal oscillator the noise power per frequency interval was much too low to be measured on the distortion analyzer. The clarity of the beat note under these conditions can be seen from Fig. 2. The video bandwidth of the presentation system was 4 mc, so that the photograph shows the total noise signal. Although no definite measurements are available, the noise level must be less than 100 db below carrier per cps.

We conclude that with reasonably decent feedback electronics, the noise arising from the fundamental crystal oscillator or the multiplier chain is negligibly small, even with a frequency multiplication ratio of 10,000. Stated another way, this means that there should be no difficulty in operating a phase stabilizer from a 10-mc crystal in the 100-kmc frequency region, and so on.

There is no doubt that the system as we have operated it is far from optimum. The IF frequency is low. This was governed by a desire to have it less than the fundamental

² M. Peter and M. W. P. Strandberg, "Phase stabilization of microwave oscillators," *Proc. IRE*, vol. 43, pp. 869-873, July, 1955.

³ F. P. Felch and J. O. Israel, "A simple circuit for frequency standards employing overtone crystals," *Proc. IRE*, vol. 43, pp. 596-603, May, 1955.

⁴ M. W. P. Strandberg, "Phase stabilization of microwave oscillators," *Proc. IRE*, vol. 44, p. 696; May, 1956.

* Received by the IRE, October 22, 1959. This work was supported in part by the U. S. Army (Signal Corps), the U. S. Air Force (Office of Scientific Research, Air Research and Development Command), and the U. S. Navy (Office of Naval Research).

¹ M. W. P. Strandberg, Letter to the Editor, *Radiotek. i Elektron.*, vol. 3, p. 1220; September, 1958.

* Received by the IRE, November 1, 1959.

¹ F. W. Hough, "AGU Committee for the Study of the Metric System in the United States," *Proc. IRE*, vol. 47, p. 584; April, 1959.

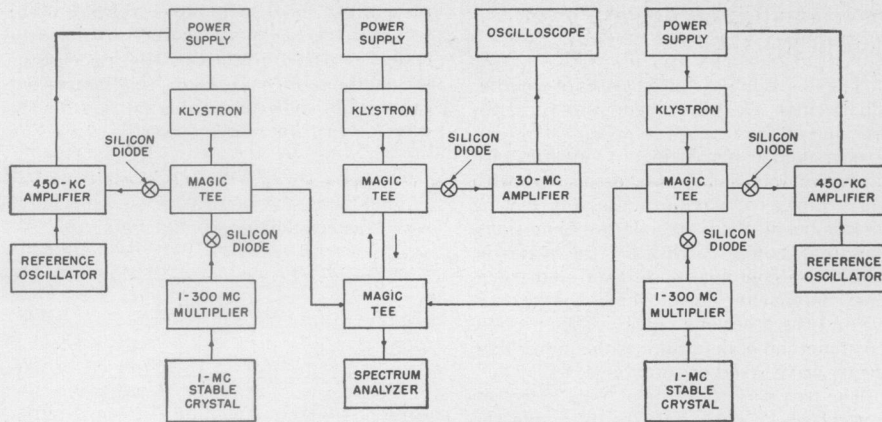


Fig. 1—Phase-locked stabilization of microwave frequencies.

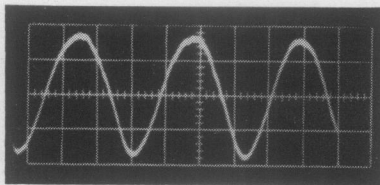


Fig. 2—Beat note of two phase-locked klystrons.

crystal-oscillator frequency. Thus the system was limited to a locking range of less than 0.5 mc; the hold in range, however, was approximately 10^4 mc. Even with this relatively poor design, these experiments have removed any doubt about the feasibility of phase-locking techniques—in the face of the argument that in the process a catastrophic amount of noise will also be generated. There is no doubt that this noise limitation will be met as the multiplication ratio becomes greater. As far as we can foresee, a multiplication ratio of 10,000 should be quite sufficient for most purposes, and should still be adequately remote from the multiplication ratio that would yield a noisy spectrum in the stabilized klystron output.

The over-all, long-time, relative phase stability of the two systems has not been studied because a study of the phase stability of the particular multipliers used would not be of general interest. The secular phase shift in the multiplier output can be reduced by limiting the number of multiplier stages and carefully controlling the input signal, temperature, operating potentials, and so forth. It would seem that a single-stage multiplier would be ideal for this purpose because it would minimize the amount of control that would have to be introduced to remove secular phase drifts from the multiplier chain. These secular drifts would only be evident if two klystrons were stabilized through two multiplier chains to a single crystal reference source, and the relative phase of each klystron with respect to the other determined. Few applications would have such stringent stability requirements. On the other hand, there are advantages in having a simple multiplier chain, simply from the point of view of convenience.

Some investigation of single-stage multipliers is being carried out in the Microwave Spectroscopy Laboratory, M.I.T. In particular, it has been pointed out by Sharp-

less⁵ that gallium arsenide shows no carrier storage effects for switching times of the order of 10^{-10} seconds. Gallium-arsenide crystals, kindly supplied by the Texas Instruments Company, are being investigated under operating conditions in which they are driven hard by a 10-mc potential into the conduction region and into the Zener breakdown region. At 10 mc, with 100-mw power at 10 mc into the crystal, we should be able to obtain $0.1 \mu\text{w}$ of power at 10,000 mc. This would be more power than is needed to obtain satisfactory low-noise phase-locking.

The author would like to acknowledge the assistance of J. G. Ingersoll in carrying out the phase-locking experiments reported here.

M. W. P. STRANDBERG
Dept. of Physics and Res. Lab. of Electronics
Massachusetts Institute of Technology
Cambridge, Mass.

⁵ W. M. Sharpless, "High-frequency gallium arsenide point-contact rectifiers," *Bell Sys. Tech. J.*, vol. 38, pp. 259–269; January, 1959.

Beam Focusing by RF Electric Fields*

It is well known that the periodic electrostatic fields can focus electron beams. One might suppose that the RF electric fields with a distribution similar to those fields can focus the beam. We studied the case of a strip beam passing through a parallel plane waveguide which carries E_{01} mode, and obtained some general conclusions.

Assumptions used are: 1) small perturbation, 2) the contribution of magnetic fields may be neglected, and 3) the term $(dy/dz)dv/dt$ may be neglected. The second assumption is reasonable if $u_0 \ll c$ and if the operating frequency is not near the cutoff points. Following the well-known procedure, one gets the path equation, eliminating t in

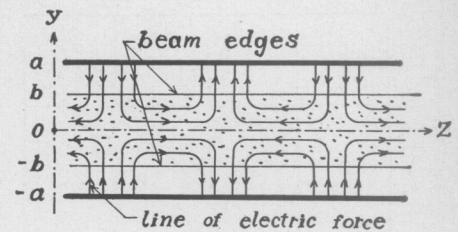


Fig. 1—Electric field distribution between two parallel planes.

the equation of motion.¹ The small perturbation from $y=b$ is expressed by

$$y_1 = q_1 \cos(\alpha z - \delta) + p_1 \sin(\alpha z - \delta),$$

$$\alpha = \frac{\omega}{u_0} + \beta, \quad \delta = \frac{\omega}{u_0} z_0. \quad (1)$$

Substituting (1) into the path equation, one gets the condition of stability.²

It is of interest that the beam can not be focused by forward traveling waves. The power required to focus the beam by backward waves, P_1 , is given by

$$P_1 = 8.02 \times 10^6 \frac{I_0}{F_1(\omega) \sin\left(\frac{b}{a} \pi\right)} \text{ (watts/m)}$$

$$F_1(\omega) = \frac{(\omega_c/\omega)^2}{1 + \frac{u_0}{c} \sqrt{1 - (\omega_c/\omega)^2}} \cdot \left[1 + \frac{u_0}{c} \frac{\sqrt{1 - (\omega_c/\omega)^2}}{1 + \frac{u_0}{c} \sqrt{1 - (\omega_c/\omega)^2}} - \frac{1}{\sqrt{1 - (\omega_c/\omega)^2}} \right]. \quad (2)$$

The magnitude of perturbation q_1/b is of the order of $3 \times 10^{-2} \pm \sqrt{I_0 a}$. In the case of standing wave focusing, the necessary power P_2 (one-directional) is

$$P_2 = 1.01 \times 10^8 \frac{I_0/\sqrt{V_0}}{F_2(\omega) \sin\left(\frac{b}{a} \pi\right)} \text{ (watts/m)}$$

$$F_2(\omega) = \left(\frac{\omega_c}{\omega}\right)^2 \frac{\{1 - (\omega_c/\omega)^2\}^{3/2}}{1 - \left(\frac{u_0}{c}\right)^2 \{1 - (\omega_c/\omega)^2\}}. \quad (3)$$

q_2/b is of the order of $0.4 \times \sqrt{I_0/\sqrt{V_0}}$. P_2 is larger than P_1 because the forward traveling waves have defocusing action. As the magnitudes of $F_1(\omega)$ and $F_2(\omega)$ are of the order of 1, P_1 and P_2 are considerably large for reasonable I_0 (A/m) (see Fig. 2). It is noted that P_1 is proportional to I_0 , while P_2 to $I_0/\sqrt{V_0}$.

The explanation for defocusing action of forward traveling waves is as follows. The electric field of E_{01} mode is given by

¹ P. K. Tien, "Focusing of a long cylindrical electron stream by means of periodic electrostatic fields," *J. Appl. Phys.*, vol. 25, pp. 1281–1288; October, 1954.

² Report presented to the Meeting of the Professional Group on Microwave Tubes of the IEE, Japan; July, 1959.

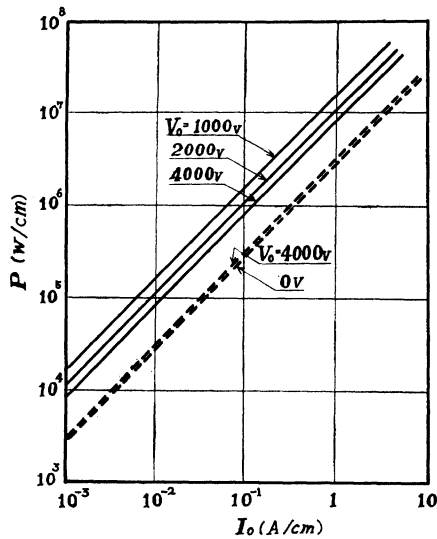


Fig. 2—Power required to focus the beam. Solid lines: power for standing waves. Dotted lines: power for backward traveling waves.

$$\begin{aligned} E_y &= \beta \sin k_y y \cos(\omega t \pm \beta z), \\ E_z &= \mp k_y \cos k_y y \sin(\omega t \pm \beta z). \end{aligned} \quad (4)$$

Putting $t=0$, (4) becomes

$$\begin{aligned} E_y &= \beta \sin k_y y \cos \beta z, \\ E_z &= -k_y \cos k_y y \sin \beta z. \end{aligned} \quad (5)$$

The field distributions of both forward and backward traveling waves are identical and similar to periodic electrostatic fields. To clarify the action of those traveling wave fields, it is helpful to see those fields from a moving coordinate that is traveling with a velocity equal to the mean velocity u_0 of electrons. Then $(\omega t \pm \beta z)$ is transformed into $(\omega/u_0 \pm \beta)z - (\omega/u_0)t$. The field distribution on the moving coordinates is obtained by substituting $\omega/u_0 \pm \beta$ into β of (5) and shifting the origin of coordinates. There are two cases: 1) $\omega/u_0 \pm \beta$ and β have the same sign or 2) they have the opposite sign. In the former case, the distribution is similar to periodic electrostatic fields. In the latter case, the phase relation between E_y and E_z is opposite to (5); electrons are axially decelerated when they experience outward force and accelerated when they experience inward force, which is contrary to the case of electrostatic lenses. In our E_{01} mode, the backward wave corresponds to the former case and the forward wave to the latter. This means the forward wave has defocusing action.

The phase relation between electric field components in slow wave circuit is the same as (5). In general, one may conclude that backward traveling waves and forward traveling waves which are slower than electrons can focus the beam, but forward traveling waves which are faster than electrons cannot.

E. SUGATA
M. TERADA
K. URA
Y. IKEBUCHI
Dept. of Electronic Engrg.
Osaka University
Higashinoda, Miyakojima
Osaka, Japan

Determination of Sign of Power Flow in Electron Beam Waves*

The question very often arises of whether a particular electron beam wave carries positive power or negative power.¹ This can be particularly perplexing in dealing with transverse waves, because, associated with every transverse wave in an axially flowing electron beam, there are axial wave motions. The total power carried by the wave is, therefore, a combination of axial and transverse components, one of which may be positive and the other one negative. We propose here a method of determining the power flow for any wave, axial or transverse.

The best way to set up a "pure" electron wave of phase velocity v_1 , is to couple the beam loosely to a circuit capable of carrying a pure wave at the same phase velocity; under this condition the circuit wave will slowly excite the beam wave. For typical electron beams, we need consider only quasi-static fields, where the phase velocity is so low that the electric fields of the wave differ negligibly from the fields of some electrostatic configuration moving at velocity v_1 with respect to a stationary observer. If we imagine ourselves moving at velocity v_1 , we see purely static periodic fields. In such fields the radial velocity perturbations imparted (eventually) to the electrons must represent energy which is equal and opposite to the axial energy change experienced by the electrons. That is, as the electrons move through the static periodic fields and develop increasing radial velocities, they have the same increase in radial energy as decrease in axial energy. If, therefore, a radial velocity \tilde{v}_r is imparted to the electrons, an axial velocity change \tilde{v}_z is likewise imparted, in such a way that the total change in the ac energy or power in the beam is zero. The beam in the coordinate system of the wave is moving to the left at velocity $(v_b - v_1)$, where v_b is the beam velocity in the laboratory coordinates. The energy relationship is

$$\tilde{v}_r^2 + (v_b - v_1 + \tilde{v}_z)^2 = (v_b - v_1)^2 \quad (1)$$

which reduces to

$$\tilde{v}_r^2 + 2\tilde{v}_z(v_b - v_1) + \tilde{v}_z^2 = 0;$$

for small signals,

$$\tilde{v}_r^2 = 2\tilde{v}_z(v_1 - v_b). \quad (2)$$

Now \tilde{v}_z the axial velocity perturbation and \tilde{v}_r the transverse velocity, are invariant with respect to the transformation from the moving coordinates to the laboratory system. Consequently, in laboratory coordinates, the total ac energy of the electrons is proportional to

$$W_{ac} = \tilde{v}_r^2 + (v_b + \tilde{v}_z)^2 - v_b^2 = \tilde{v}_r^2 + 2v_b\tilde{v}_z. \quad (3)$$

(for small signals). Substituting from (2) we obtain

$$W_{ac} = \tilde{v}_r^2 + \tilde{v}_r^2 \frac{v_b}{v_1 - v_b} = \tilde{v}_r^2 \left(\frac{v_1}{v_1 - v_b} \right). \quad (4)$$

The "sign" of the ac power carried by the beam will be the same as the sign of W_{ac} . The relative proportion of axial and transverse

power can also be obtained from (4). The factor \tilde{v}_r^2 is always positive so that the energy imparted to the electrons depends on the factor $(v_1/v_1 - v_b)$. From this factor, one can readily show that the condition for the wave to carry negative power is

$$v_b/v_1 > 1. \quad (5)$$

The phase velocities of space charge waves and cyclotron waves are given by

$$\begin{aligned} v_1(\text{space charge}) &= \frac{v_b}{1 \pm \frac{\omega_p}{\omega}}, \\ v_1(\text{cyclotron}) &= \frac{v_b}{1 \pm \frac{\omega_c}{\omega}}. \end{aligned}$$

where in general, ω_p and ω_c have values depending on the beam geometry, as is well known. From (5), the slow space charge wave and the "slow" cyclotron wave both have negative power flow.

W. R. BEAM
Rensselaer Polytech. Inst.
Troy, N. Y.

Response of a Square Aperture to a Thermal Point Source of Radiation*

Antenna patterns are defined for point-source continuous wave targets. In these days of radio astronomy and thermal ground mapping, however, it is of interest to show the effective antenna pattern against a black body point source. It is evident from the start that an increase in bandwidth will receive more power, but produce some progressive pattern change from the familiar cw pattern.

Power radiated from a black body in the radio spectrum is given by the Rayleigh Jeans' approximation to Planck's radiation formula.¹

$$\frac{dP}{A_T d\lambda} = \frac{2\pi ckT}{\lambda^4} \frac{\text{power}}{\text{unit area} \cdot \text{unit wavelength}} \quad (1)$$

where

A_T = projected area of source visible to antenna

λ = wavelength of radiation

k = Boltzmann's constant energy per degree of temperature

T = absolute temperature

c = velocity of light

An antenna is sensitive to only one polarization and thus can collect only half of this amount of power.

$$\frac{dP}{A_T d\lambda} = \pi ck \frac{T}{\lambda^4} = 1.3 \times 10^{-11} \frac{T}{\lambda^4} \frac{\text{watts}}{\text{meter}^2} \quad (2)$$

with λ expressed in meters, and T expressed in degrees Kelvin.

An antenna removed from the source a distance ρ and having an effective aperture

* Received by the IRE, November 12, 1959.

¹ The "negative power" concept was first introduced by L. J. Chu. It is of great importance in gain and noise considerations.

* Received by the IRE, November 9, 1959.

¹ R. A. Smith, F. E. Jones, R. P. Chasmar, "The Detection and Measurement of Infrared Radiation," Oxford University Press, London, England, p. 27; 1957.

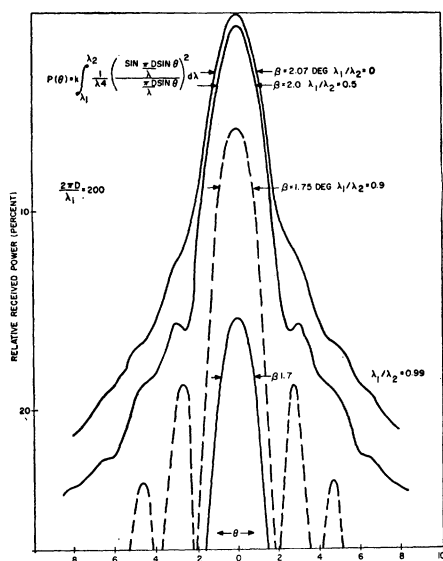


Fig. 1

of A_r receives power,

$$P = \frac{A_T \pi c k T}{4\pi \rho^2} \int_{\lambda_1}^{\lambda_2} \frac{A_r}{\lambda^4} d\lambda. \quad (3)$$

The effective area, A_r , is, in general, frequency-sensitive and depends upon the antenna design and target angle relative to the antenna. A square aperture uniformly illuminated would produce²

$$A_r(\theta\lambda) = A \left[\frac{\sin\left(\frac{\pi a}{\lambda} \sin \theta\right)}{\left(\frac{\pi a}{\lambda} \sin \theta\right)} \right]^2 \quad (4)$$

where the physical area $A = a^2$.

The reason for the selection of a square aperture is that this allows integration of (3) and just as ably demonstrates the effect as does a circular aperture which must be machine evaluated. Carrying this out, one finds

$$P = \frac{A_T c k T A}{4\rho^2} \left[\sin\left(\frac{2\pi a}{\lambda_2} \sin \theta\right) - \frac{2\pi a}{\lambda_2} \sin \theta - \sin\left(\frac{2\pi a}{\lambda_1} \sin \theta\right) + \frac{2\pi a}{\lambda_1} \sin \theta \right] \quad (5)$$

Notice that in the limit at $\theta \rightarrow 0$ (target on the antenna axis)

$$P = \frac{A_T c k T A}{4\rho^2} \frac{1}{3} \left(\frac{1}{\lambda_1^3} - \frac{1}{\lambda_2^3} \right). \quad (6)$$

Using this as a normalization with $\lambda_2 = 0C$, the relative power pattern may be written

$$p = \frac{\sin\left(\frac{2\pi a}{\lambda_2} \sin \theta\right) - \frac{2\pi a}{\lambda_2} \sin \theta}{\frac{1}{6} \left(\frac{\lambda_2}{\lambda_1}\right)^3 \left(\frac{2\pi a}{\lambda_2} \sin \theta\right)^3} \quad (7)$$

² S. Silver, "Microwave Antenna Theory and Design," Radiation Laboratory Series, vol. 12, McGraw-Hill Book Co., Inc., New York, N. Y.

Eq. (7) is shown in Fig. 1 (on the left) for $\lambda_1/\lambda_2 = 0, 0.5, 0.9, 0.99$ or, to say this another way, for an infinite, octave, ten per cent, one per cent bandwidth. With increasing bandwidth the slightly increasing beamwidth and lowering of the sidelobe levels should be noticed. Eventually, the lobes as such disappear. It is also of interest that for a given upper-frequency limit, once an octave bandwidth has been achieved only about 12 per cent more power is available by extending this to zero low frequency limit.

M. S. WHEELER
Air Arm
Westinghouse Electric Corp.
Friendship Internat. Airport
Box 746, Baltimore 3, Md.

A Dispersionless Dielectric Quarter Wave Plate in Circular Waveguide*

Certain applications of circularly polarized waves at microwave frequencies require that the axial ratio of the wave approach unity (0 db) as closely as possible and maintain this value over a broad band of frequencies. Previous applications had permitted the use of quarter wave plates which generated circularly polarized waves having an axial ratio of as much as 3 db. This note describes an improved dielectric quarter wave plate for circular waveguide which generates a circularly polarized wave with an axial ratio under 0.2 db over the 12 per cent frequency band from 8.5 to 9.6 mc.

It is well known that a circularly polarized wave can be generated by loading a waveguide of circular or square cross section with a slab of dielectric material in such a manner that equal-amplitude orthogonal waves experience a 90° differential phase

in circular waveguide have been arrived at largely on an empirical basis because of the difficulty in obtaining exact solutions for the circular waveguide case.^{1,4}

It is possible, however, to apply analytical techniques to the problem of dispersionless dielectric quarter wave plates if the parameters of desired differential phase shift, frequency limits and waveguide size are fixed and dominant mode propagation is assumed throughout. For these conditions, the solution obtained is specific rather than general and a design must be calculated for each set of parameters of interest. The method evolves from a consideration of the expression of the differential phase shift $\Delta\phi$ in a dielectric slab loaded waveguide

$$\Delta\phi = 2\pi l \left(\frac{1}{\lambda_p} - \frac{1}{\lambda_t} \right), \quad (1)$$

where λ_p is the guide wavelength existing in the waveguide when the slab is parallel to the plane of the E vector, and λ_t is the guide wavelength produced when the slab is transverse to the E vector. Using the definition for guide wavelength

$$\lambda_g = \frac{\lambda}{\sqrt{\epsilon - \left(\frac{\lambda}{\lambda_c}\right)^2}}, \quad (2)$$

(1) may be rewritten

$$\Delta\phi = \frac{2\pi l}{\lambda} \left[\sqrt{\epsilon_p - \left(\frac{\lambda}{\lambda_c}\right)^2} - \sqrt{\epsilon_t - \left(\frac{\lambda}{\lambda_c}\right)^2} \right], \quad (3)$$

where ϵ_p and ϵ_t are effective dielectric constants required to satisfy (2) for measured values of λ_p and λ_t . The effective dielectric constant will be smaller than the dielectric constant of the material employed since a waveguide partially filled with a dielectric material will have the same phase delay as a waveguide completely filled with a material of lower dielectric constant.

The dispersion D in a differential phase shift device may be defined as

$$D = \Delta\phi_1 - \Delta\phi_2, \quad (4)$$

where $\Delta\phi_1$ and $\Delta\phi_2$ are the differential phase shifts occurring, respectively, at f_1 and f_2 , the frequency limits of interest. Assuming a given waveguide size and frequency band, and setting $\Delta\phi_1 = 90^\circ$, the expression for dispersion about 90° differential phase shift becomes

$$D_{90} = \frac{\pi}{2} \left[1 - \frac{\lambda_1}{\lambda_2} \left(\frac{\sqrt{\epsilon_p - (\lambda_2/\lambda_c)^2} - \sqrt{\epsilon_t - (\lambda_2/\lambda_c)^2}}{\sqrt{\epsilon_p - (\lambda_1/\lambda_c)^2} - \sqrt{\epsilon_t - (\lambda_1/\lambda_c)^2}} \right) \right]. \quad (5)$$

Eqs. (3) and (5) were evaluated for the frequency band from 8500 to 9600 mc, assuming a 15/16-inch ID circular waveguide. In order to systematize the computation, ϵ_p and ϵ_t were chosen according to a regular progression of both the mean effective dielectric constant ϵ_m and the ratio of effective dielectric constants ρ where

⁴ R. A. Brown and A. J. Simmons, "Dielectric Quarter Wave and Half Wave Plates in Circular Waveguide," Naval Res. Lab., Washington, D. C., Rept. No. 4218, November 10, 1953.

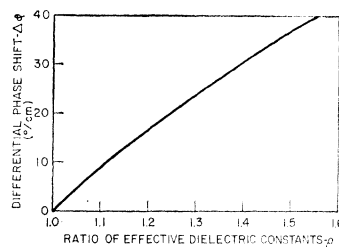
* Received by the IRE, October 19, 1959.
¹ W. P. Ayres, "Broadband Quarter Wave Plates," Electronic Defense Lab., Mountain View, Calif., Tech. Memo. No. EDL-M46; September 30, 1955.
² "Antenna Phenomena Research," Antenna Lab., Dept. of Electrical Engrg., Res. Foundation, Ohio State University, Columbus, Final Engrg. Rept. No. 594-7; November 1, 1955.
³ H. S. Kirschbaum and S. Chen, "A Method of Producing Broadband Circular Polarization Employing an Anisotropic Dielectric," Antenna Lab., Dept. of Electrical Engrg., Res. Foundation, Ohio State University, Columbus, Engrg. Rept. No. 662-2; July 16, 1956.

$$\epsilon_m = \sqrt{\epsilon_p \epsilon_t} \quad \text{and} \quad \rho = \frac{\epsilon_p}{\epsilon_t} \quad (6)$$

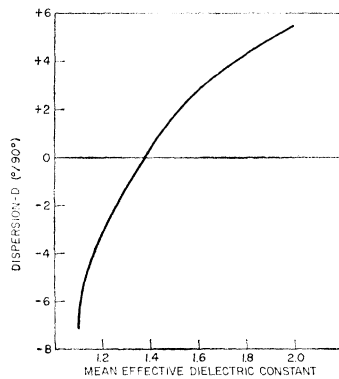
The results of the computations are shown in Figs. 1(a) and 1(b). For the conditions chosen, the differential phase shift turns out to be solely a function of ρ and the dispersion is dependent only upon the value of ϵ_m . These curves, applied to the experimental measurements of ϵ_p and ϵ_t for various thicknesses of both polystyrene and teflon, resulted in plots of differential phase shift [Fig. 2(a)] and dispersion [Fig. 2(b)] as a function of dielectric slab thickness. Note that for the assumed case, minimum dispersion occurs in the region of high differential phase shift.

In designing a dispersionless quarter wave plate on the basis of these curves, consideration must, of course, be given to proper impedance matching. Only a stepped matching structure was considered in order to calculate the dispersion and differential phase shift occurring in the matching section. Using polystyrene of sufficient thickness to give a positive dispersion (3/16 inch in this case), steps were calculated to yield a binomial impedance change in the plane of the slab. Because of the thinness of the slab, it was hoped and borne out by subsequent measurements that no special matching measures would be required in the plane perpendicular to the slab. After calculating the differential phase shift introduced by the matching section, the length of the body of the quarter wave plate was computed to produce an over-all differential phase shift of 90°. Dispersion in the design was calculated to be about 1°.

Model quarter wave plates were constructed according to the calculated di-



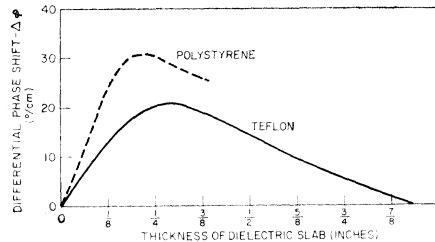
(a)



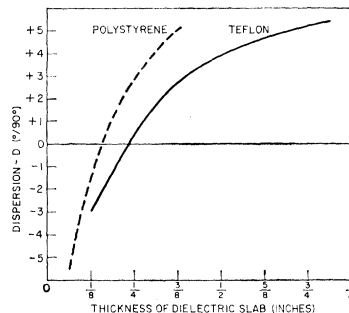
(b)

Fig. 1—(a) Differential phase shift vs ratio of effective dielectric constants for 15/16-inch ID circular waveguide at 8.5 kmc. (b) Dispersion about 90° vs mean effective dielectric constant for 15/16-inch ID circular waveguide in the frequency range 8.5 to 9.6 kmc.

mensions using both polystyrene and Rexolite, a material whose dielectric constant is the same as that of polystyrene. Axial ratios of between 0.2 and 0.3 db over



(a)



(b)

Fig. 2—(a) Differential phase shift vs thickness of dielectric slab at 8.5 kmc. (b) Dispersion about 90° vs thickness of dielectric slab.

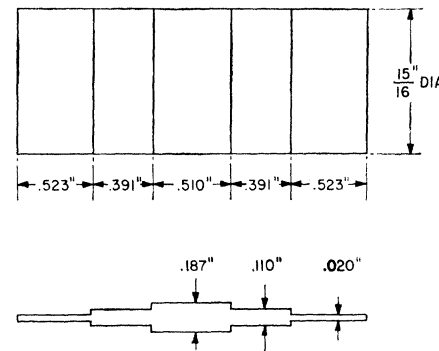
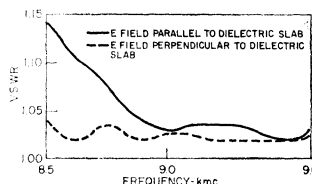
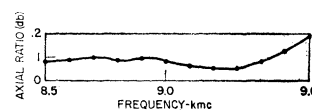


Fig. 3—A dispersionless quarter wave plate showing dimensions in inches. Material is polystyrene.



(a)



(b)

Fig. 4—(a) VSWR vs frequency for E field parallel and perpendicular to dielectric slab. (b) Output axial ratio of quarter wave plate.

the 12 per cent frequency band were obtained. Subsequent measurements indicated that the differential phase shift was slightly in excess of the desired 90°. By shortening the body of the dielectric element 0.015 inch, the error in the differential phase shift was reduced and a quarter wave plate which generates a circularly polarized wave of less than the 0.2-db axial ratio was obtained. This is within 2 per cent of perfect circular polarization. The dimensions of the final model, designed to fit in 15/16-inch ID circular waveguide, are shown in Fig. 3, and the electrical performance characteristics of the unit are shown in Figs. 4(a) and 4(b).

R. D. TOMPKINS
Radar Division
Naval Research Lab.
Washington 25, D. C.

Measuring the Mean Square Amplitude of Fading Signals Using a Selected Quantile Output Device (SQUOD)*

In many experiments it is necessary to measure the mean-square amplitude of a varying signal. The use of a square law detector is obvious. However, if the mean amplitude varies over a wide range, a system of attenuators has to be used, which is a disadvantage in automatic equipment designed to measure the signal over long periods.

The ideal receiver for measuring the amplitude of a signal which may vary over a wide range is one with a logarithmic characteristic such as that described by Chambers and Page.¹ The mean output from such a receiver does not, however, correspond to the root mean square signal. When the fading is completely random, for instance, the mean output is about 9 db in power below that corresponding to the rms signal.

The purpose of this note is to draw attention to the fact that, if the signal input to a nonlinear receiver consists of steady and random components as described by Rice,² then the quantile of the output voltages, chosen so that the receiver output is less than the quantile for 60 per cent of the time, is almost equal to the output corresponding to the rms-signal input. This is shown in Fig. 1 where the error in decibels, by which the input signals corresponding to the various quantiles exceed the rms-signal input, is plotted against the ratio of the square of the amplitude of the random component to the mean-square value of the signal, a measure of the depth of fading. It is seen that the quantile chosen leads to an error of less than 0.26 decibel, no matter what the depth of fading.

A device called a "Selected Quantile Output Device," or SQUOD, has been con-

* Received by the IRE, December 1, 1959.

¹ T. H. Chambers and I. H. Page, "The high-accuracy logarithmic receiver," *Proc. IRE*, vol. 32, pp. 1307-1314; August, 1954.

² S. O. Rice, "Mathematical analysis of random noise," *Bell Sys. Tech. J.*, vol. 23, pp. 282-332, July, 1944; and vol. 24, pp. 46-156, January, 1945.

structed for determining the required quantile. The circuit, shown in Fig. 2, includes an amplitude comparator—the first ECC81—between the voltage input from the receiver and output to the recorder. The input voltage is a dc negative-going voltage varying from +20 to -20 volts. The adaption of the circuit to positive-going voltages is obvious.

The comparator operates a relay. With the relay closed or open, the condenser C (12 mf) charges or discharges through the resistance R , at uniform rates determined by the 15-volt or 22-volt batteries respectively, with R_2 (approximately 300 Ω) providing a fine control. The electrometer tube 4066 is used in a circuit basically due to Farmer.³ The grid current is about 10^{-12} amp, allowing values of R up to about 10^{10} ohms. The voltage on the condenser C is thus transferred to the grid of the last half of the second ECC81, which acts as a cathode follower with a constant current load. As the battery voltages are fixed relative to the output voltage, the charging and discharging rates remain fixed.

The OA81 diode connected to the anode of the first ECC81 insures that, should the input voltage drop and the second half of the tube take all the current, the second anode cannot drop much below 85 volts and cannot force its grid to draw current.

The 4-mf condenser shunts the output of the electrometer tube and removes all ripple caused by fluctuating emission of the filament. This capacitive shunt path is taken via the condenser C , in order to mini-

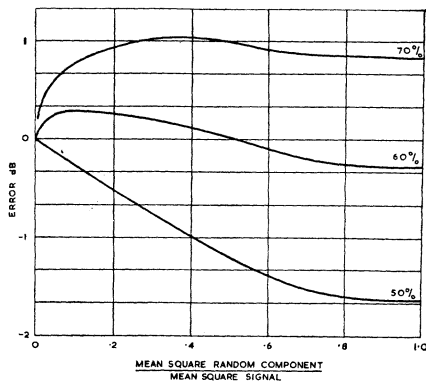


Fig. 1—The error in decibels by which the various quantile exceed the rms value, plotted against the ratio of the mean square value of the random component to the mean square value of the signal when the selected quantile exceeds the signal for 50, 60, and 70 per cent of the time.

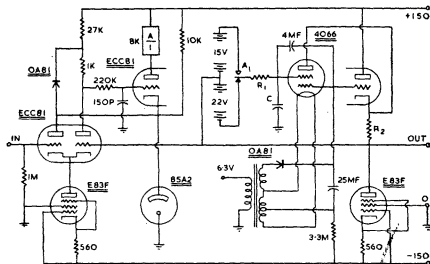


Fig. 2—Circuit of the SQUOD.

³ F. T. Farmer, "Electrometer for measurement of voltages on small ionization chambers," *Proc. Phys. Soc.*, vol. 54, pp. 435-438; September, 1942.

mize phase lag in the control loop. As the electrometer tube has a gain of approximately one, the capacity seen in shunt with C from R is negligible.

The device is sensitive to changes of input voltages of 0.05 volt, and has a working range of about 60 volts.

The SQUOD, in conjunction with the logarithmic receiver, is being used for automatic and accurate recording of the mean-square amplitude of echoes reflected from the ionosphere, and may be of use in other applications in which quantities to be measured are subject to random fluctuations.

The authors gratefully acknowledge the receipt of research grants from the University of New Zealand.

A. E. ADAM
J. D. WHITEHEAD
Physics Department
University of Otago
Dunedin, New Zealand

Observations on Angle Diversity*

Recently several papers have appeared discussing the use of angle diversity^{1,2} in a tropospheric scatter system. These papers suggest that, at the upper UHF and SHF bands, angle diversity is much more efficient than any other type of diversity. It is the purpose of this note to attempt to clarify the characteristics of angle diversity, and to point out that it is probably no better than simple space diversity from S/N points of view and that the total real estate required is also the same. Angle diversity, however, will provide greater bandwidth capability because the very narrow beams utilized will cut down multipath delays.

To be specific, let us consider the analysis presented by Vogelmann, *et al.*² They suggest the use of a very large antenna with multiple feeds at the transmitting end to illuminate the entire effective scatter volume with non-overlapping beams (measured by the 3 db points). By implication, each of the beams would illuminate only a fraction of that volume. Thus, if five feeds were used, each beam would illuminate approximately one-fifth of the effective scatter volume. Let us pursue the implication of this a little further by considering two cases. In each case, the total power output at the transmitter is the same. In one case, the power is split among the several feeds in a large antenna. In the other case, all the power is put into one smaller antenna whose beam fills the same volume as all the beams of the larger antenna do. Since the total power being fed in at the transmitting end is the same for both situations and the volume through which the power flows is also the same the power,

density flux through the scatter volume must be the same for both cases. It would appear, therefore, that in general it would be preferable to put all the power into one feed of a smaller antenna than to use a complex arrangement of multiple feeds and multiple frequencies in a large antennas as has been suggested.² One qualification must be added. If the required total power output is many times the power output capability of a single tube, then the paralleling of many tubes at the transmitter may also become a difficult problem. However, to offset this difficulty, we have the following advantages: 1) paralleling several tubes is more efficient in terms of radiated power because the off-centering of the multiple feeds involves a loss of probably 3 to 6 db per feed; 2) the alignment of the larger beam associated with the smaller antenna becomes simpler; and (3) much less bandwidth is required.

Now let us consider the receiving end. If multiple feeds are placed in one large antenna, angle diversity could be achieved. However, the same S/N statistics can be achieved by the more conventional means of spaced smaller antennas and, moreover, the total real estate required would be the same for both cases. To make this clear, consider an antenna whose beamwidth just fills the effective scattering volume. In this discussion this antenna will be called the reference antenna. This antenna will realize its full free-space gain. Any larger antenna will suffer an antenna-to-medium coupling loss such that the received signal would be of comparable magnitude to the signal received on the reference antenna. Thus an antenna which has five times the area of the reference antenna will "see" approximately one-fifth of the effective scatter volume. A corollary to this is that phase coherence of the incoming wave is not maintained over the dimensions of this larger antenna. As a matter of fact, the phase of the incoming wave is coherent over an area approximately one-fifth that of the antenna itself. This means that we can place five smaller antennas, each the size of our reference antenna, in a diversity system in the same area occupied by the larger antenna, and as already stated, each of these smaller antennas will receive a signal of magnitude comparable to that received by the larger antenna. Thus, from this example we see that the one large antenna (five times the area of our reference antenna) which utilizes five different feeds arranged for diversity will give the same S/N statistics as five antennas each the size of our reference antenna. Also, the area occupied by either antenna system is the same. As mentioned at the beginning of this letter, the one advantage that a system utilizing a larger antenna with multiple feeds has is greater bandwidth capability. However, to achieve this angle diversity for the purpose of increasing bandwidth capability, one does not have to utilize multiple feeds and multiple frequencies in a large antenna at the transmitting end. One smaller antenna whose beam just fills the effective scatter volume will suffice.

HAROLD STARAS
RCA Labs.
Princeton, N. J.

* Received by the IRE, November 2, 1959.
¹ R. Bolgiano, Jr., N. H. Bryant, and W. E. Gordon, "Diversity Research in Scatter Communications with Emphasis on Angle Diversity," Contract AF 30(602)-1717, Final Rept., pt. I, January, 1958.
² J. H. Vogelmann, J. L. Ryerson, and M. H. Bickelhaupt, "Tropospheric scatter system using angle diversity," *Proc. IRE*, vol. 57, pp. 688-696; May, 1959.

Author's Comment³

Mr. Staras in his communication "Observations on Angle Diversity" has assumed that the purpose of this type of diversity is to illuminate the entire scatter volume with a uniform power density flux. I would like to point out that this is not the case. The purpose of angle diversity is to increase the reliability of tropospheric scatter communications. To this end, let me illustrate the advantages of angle diversity with numerical values rather than by pointing out flaws in Mr. Staras' letter.

Using Mr. Staras' illustration, let us compare the following two cases:

Case I. A 30-foot antenna with 4 units arranged for space diversity in the same geographic area as Case II; two antennas over two. Power per reflector is the same as power per feed in Case II. The frequency is 10 kmc.

Case II. A 60-foot antenna with 4 feeds in a row at 0° elevation. Power per feed is the same as power per reflector in Case I. The frequency is 10 kmc.

The distance between transmitter and receiver is 300 miles; Realized Gain⁴ per antenna pair (1 receive and 1 transmit) for Case I is 86 db; and Realized Gain per beam pair (1 receive and 1 transmit) for Case II is 89.2, 89.9, 89.9, and 89.2, respectively. Using 50 per cent reliability for one path of Case I, identical transmitter power and receiver sensitivity, the reliabilities for the individual beams of Case II are 75 per cent, 80 per cent, 80 per cent and 75 per cent respectively.⁵

With quadruple space diversity, Case I gives an over-all reliability of 88 per cent or 120 errors per 1000, while 4 feed angle diversity gives in Case II an over-all reliability of 99.7 per cent or 3 errors per thousand.

JOSEPH H. VOGELMAN
Dynamic Electronics Div.
Capehart Corp.
Richmond Hill 18, N. Y.

³ Received by the IRE, December 4, 1959.
⁴ L. P. Yeh, "Tropospheric Scatter System Design," Westinghouse Electric Corp., Baltimore, Md., Tech. Rept. No. 5; October, 1957. See Fig. 4.
⁵ *Ibid.*, Fig. 6.

General *N*-Port Synthesis with Negative Resistors*

This note gives an *n*-port synthesis for any *n* × *n* admittance [*Y*(*p*)], impedance [*Z*(*p*)], or scattering [*S*(*p*)], matrix, in which the matrix elements are general rational functions with real coefficients containing zeros and poles of arbitrary multiplicity anywhere in the complex frequency (*p*) plane. It will be shown that the synthesis can always be performed with passive

elements (*R*, *L*, *C*, gyrators, ideal transformers) and negative resistors. This total group will here be defined as "physical elements."

First consider the synthesis of *Y*(*p*). Express each element $y_{ij}(p) = \sum a_k p^k + y_{ij}^{(0)}(p)$ where $y_{ij}^{(0)}(p)$ is a proper fraction and hence has no poles at ∞. Then $Y(p) = \sum p^k A_k + Y_0(p)$, where the *A*_{*k*} are real constant matrices. Let us consider the synthesis of one of the matrices $p^k A_k$. *A*_{*k*} may be separated into its symmetric (*A*_{*k*}[']) and skew symmetric (*A*_{*k*}^{''}) parts, and each of these diagonalized by a real congruent transformation. The symmetric part $p^k A_k''$ goes into diag (*p*^{*k*}, *p*^{*k*}, . . . , 0_{*m+1*}, . . . , 0_{*n*}) where the rank of *A*_{*k*}['] is *r*. The skew symmetric part, $p^k A_k'$, goes into

$$\text{diag} \cdot \begin{bmatrix} 0 & p^{-k} \\ p^k & 0 \end{bmatrix}, 0_{m+1}, \dots, 0_n$$

where the rank of *A*_{*k*}['] is *m*, an even number. Each 0_{*j*} is a scalar zero. We have then merely to show the synthesis of the diagonal elements

$$\pm p^k, \begin{bmatrix} 0 & -p^k \\ p^k & 0 \end{bmatrix},$$

and by appropriate transformers and parallel interconnections¹ $\sum p^k A_k$ may be synthesized as an *n*-port.

Fig. 1 shows how the admittance element $\pm p^2$ is synthesized; and in conjunction with the negative impedance converter circuit of Fig. 2, it is clear that $\pm p^2$ only requires passive elements and negative resistors. Fig. 3 shows how the admittance $\pm p^{n+1}$ can be synthesized in terms of elements of lower degree. Hence, by induction any p^k may be constructed of physical elements. Fig. 4 shows the realization of the admittance matrix

$$\begin{bmatrix} 0 & -p^k \\ p^k & 0 \end{bmatrix}$$

in terms of physical elements, where the admittance element $\pm p^k$, synthesized above, is used as a building block.

The next step is to synthesize *Y*₀(*p*), whose singularities are all in the finite *p* plane. Let σ₀ be the positive real part of that pole of *Y*₀(*p*) located farthest to the right of *j*ω in the complex *p* plane. Then make the frequency transformation $s = p - \tau$, $\tau > \sigma_0$. The function *Y*₀(*s*) is now analytic on *j*ω and in the right half *p* plane, though it need not be passive (*i.e.*, it need not possess a positive quadratic form for internally dissipated power). The synthesis of such a *Y*(*s*) has been given previously as a passive network some of whose ports are augmented by series-connected negative resistors.¹ Each coil *L* in the network for *Y*₀(*s*) is now replaced by the series combination of *L* and a negative resistor $-L\tau$, and each condenser *C* by *C* in parallel with negative conductance $-C\tau$. This gives *Y*₀(*p*) as a network with physical elements, and the parallel combination of *Y*₀(*p*) with $\sum p^k A_k$ completes the synthesis.

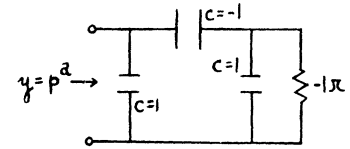


Fig. 1.

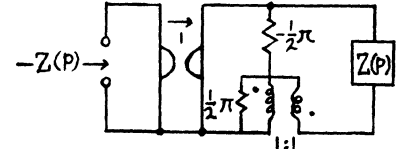


Fig. 2.

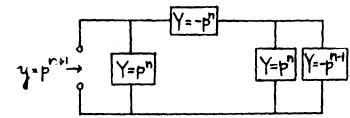


Fig. 3.

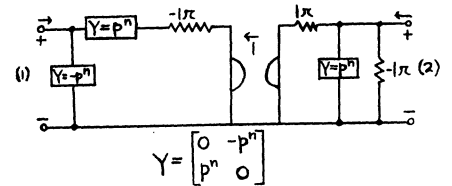


Fig. 4.

It is clear that *Z*(*p*) may be synthesized by a dual process.

Suppose now that *S*(*p*) is specified, and neither the *Z*(*p*) nor *Y*(*p*) representations corresponding to this *S* exists. Since *S* exists, the admittance matrix *Y*_{*A*} of an augmented network exists,² corresponding to the network for *S*(*p*) with a unit positive resistor added in series to each port. $Y_A = \frac{1}{2}(I - S)$. *Y*_{*A*}(*p*) is synthesized as described above to give the augmented network *N*_{*A*}. To find *N* corresponding to *S*, we "de-augment" *N*_{*A*} by adding -1 ohm resistors to each port of *N*_{*A*}. No attempt has been made to minimize the number of elements, but the synthesis given proves the general theorem:

Any *n* × *n* scattering matrix of rational real functions of *p* can be represented by a linear, time invariant, lumped *n*-port network containing only passive elements and negative resistors.

The number of resistors can be reduced by the following technique. Consider *Y*(*p*) and suppose all boundary poles have been removed, so that *Y*(*j*ω) is bounded. Simple poles on $p = j\omega$ with positive residue matrices are removable as passive lossless networks, and higher-order boundary poles as well as simple boundary poles with non-positive residue matrices are synthesized by a simple modification of the technique given above in connection with Figs. 1-4. Write $Y(p) = Y_1(p) + Y_2(p)$, where, by combining appropriate terms of a partial fractions expan-

* Received by the IRE, November 20, 1959. This work was done under Contract AF-18(600)-1505 sponsored by the Army, Navy and Air Force.

¹ H. J. Carlin, "The synthesis of non-reciprocal networks," *Proc. Symp. on Modern Network Synthesis II*, Polytechnic Institute of Brooklyn, Brooklyn, N. Y., vol. 5, pp. 11-44; April, 1955.

² H. J. Carlin, "The scattering matrix in network theory," *IRE TRANS. ON CIRCUIT THEORY*, vol. CT-3, pp. 88-97; June, 1956.

sion, $Y_1(p)$ has only left-half p -plane poles and $Y_2(p)$ has only right-half p -plane poles. Now $Y(p) = \hat{Y}_1(p) + \hat{Y}_2(p)$, where $\hat{Y}_1(p) = G + Y_1(p)$, $\hat{Y}_2(p) = -G + Y_2(p)$. $G = \text{diag}(g_1, g_2, \dots, g_n)$ where the g_k are all real, non-negative, and may be chosen equal to each other, with g_k the maximum value required to make $\hat{Y}_1(p)$ and $-\hat{Y}_2(-p)$ positive real matrices. This can always be done with a real finite g_k since $Y(j\omega)$ is bounded, and $\hat{Y}_1(p)$ and $-\hat{Y}_2(-p) = G - Y_2(-p)$ are both analytic in the right half of the p plane.¹ The positive real matrix $\hat{Y}_1(p)$ may always be synthesized as a passive network containing at most n resistors all positive. By a theorem of Youla,² if $-\hat{Y}_2(-p)$ is PR , then $\hat{Y}_2(p)$ may be synthesized as a network containing lossless elements plus at most n resistors, all negative. Combining $\hat{Y}_1(p)$ and $\hat{Y}_2(p)$ in parallel gives $Y(p)$. Utilizing duality, we may state the following general theorem.

Any $n \times n$ immittance matrix of rational functions, which has no boundary ($p = j\omega$) poles other than those of simple order with non-negative residue matrices at these boundary poles, may be synthesized as an n -port network containing only lossless elements and at most n -positive and n -negative resistors.

A driving point impedance of the above type, for example, requires at most one positive resistor and one negative resistor.

H. J. CARLIN
Microwave Res. Inst.
Polytechnic Inst. of Brooklyn
Brooklyn, N. Y.

¹ Microwave Res. Inst., Polytechnic Institute of Brooklyn, Brooklyn, N. Y., MRI Quarterly Rept. No. 16, R-452.16-59, pp. 55-56; April 15, 1959. Contract No. AF-18(600)-1505.

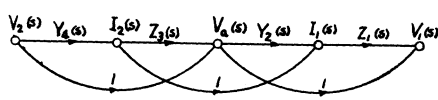


Fig. 1—A signal flow graph method for determining ladder network functions.

There are no feedback paths, so the determinant has a value of unity. The following relations may then be written by inspection³ (if it is remembered that any node may be treated as a sink).

$$\frac{V_1(s)}{V_2(s)} = Y_4(s)Z_3(s)Y_2(s)Z_1(s) + Y_4(s)Z_3(s) + Y_4(s)Z_1(s) + Y_2(s)Z_1(s) + 1, \quad (6)$$

$$\frac{I_1(s)}{V_2(s)} = Y_4(s)Z_3(s)Y_2(s) + Y_4(s) + Y_2(s), \quad (7)$$

$$\frac{I_1(s)}{V_2(s)} = Y_4(s). \quad (8)$$

From these,

$$Z_{in}(s) = V_1(s)/I_1(s) = (6) \text{ divided by } (7);$$

$$I_2(s)/I_1(s) = (8) \text{ divided by } (7);$$

$$V_2(s)/V_1(s) = \text{the reciprocal of } (6);$$

$$Z_{21}(s) = V_2(s)/I_1(s) = \text{the reciprocal of } (7).$$

Thus, all the network functions may be obtained by inspection of one graph.

The form of the result is slightly different from that given by Kuo and Leichner, and the relative convenience or shortness of the methods may depend on the particular problem, and on the types of immittance involved.

G. H. BURCHILL
Nova Scotia Tech. College
Halifax, Nova Scotia

² S. J. Mason, "Feedback theory—further properties of signal flow graphs," Proc. IRE, vol. 44, pp. 920-926, July, 1956.

A Signal Flow Graph Method for Determining Ladder Network Functions*

An iterative method for determining ladder network functions was described by Kuo and Leichner,¹ with the suggestion that the signal flow method was not very convenient. For comparison, a signal flow solution is presented here.

Using the same circuit as Kuo and Leichner, a ladder with series impedances $Z_1(s)$ and $Z_3(s)$ and shunt admittances $Y_2(s)$ and $Y_4(s)$, and the same equations written in their simplest forms,

$$V_2(s) = V_1(s), \quad (1)$$

$$I_2(s) = Y_4(s)V_2(s), \quad (2)$$

$$V_a(s) = I_2(s)Z_3(s) + V_2(s), \quad (3)$$

$$I_1(s) = Y_2(s)V_a(s) + I_2(s), \quad (4)$$

$$V_1(s) = I_1(s)Z_1(s) + V_a(s), \quad (5)$$

a signal flow graph may be drawn (Fig. 1).

* Received by the IRE, November 2, 1959.
¹ F. F. Kuo and G. H. Leichner, "An iterative method for determining ladder network functions," Proc. IRE, vol. 47, pp. 1783-1784; October, 1959.

A Different Approach to the Approximation Problem*

The response curves that are usually desired in network theory cannot be exactly

$$Z = \frac{R\sqrt{\epsilon}}{\sqrt{1 + \left(\frac{s}{\omega_0}\right)^2} \exp\left[\frac{1}{2}\left(\frac{s}{\omega_0} \arctan \frac{\omega_0}{s} + \frac{\omega_0}{s} \arctan \frac{s}{\omega_0}\right)\right]} \quad (4)$$

synthesized. A reasonable approximation to the desired response is therefore made and the corresponding network is synthesized. Where an infinite number of "reasonable approximations" exist, there are an infinite number of solutions to the problem.

It is possible to follow a less arbitrary approach, based upon the fact that a physically realizable response curve can be expressed as an exact function of s , where $s = j\omega$. Consider the amplitude and phase

* Received by the IRE, October 27, 1959. This work was supported in part by the Office of Naval Research under Contract Nonr-839(05).

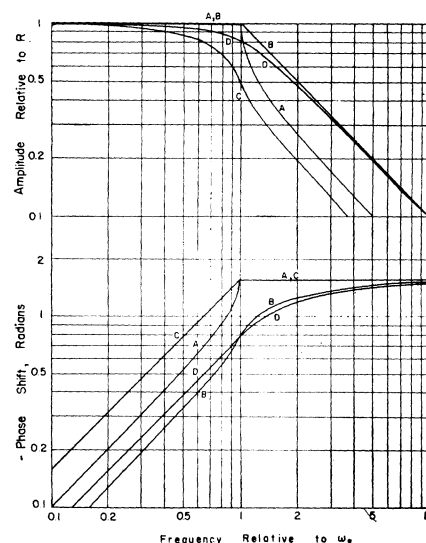


Fig. 1—Various "ideal" response curves.

responses of curves A to D in Fig. 1, where ω_0 is a nominal cutoff frequency.

For curve A, the amplitude response is flat up to ω_0 while the phase response is flat beyond ω_0 . It is described by¹

$$Z = \frac{R}{\frac{s}{\omega_0} + \sqrt{1 + \left(\frac{s}{\omega_0}\right)^2}} \quad (1)$$

For curve B, the amplitude response is flat up to ω_0 and decreases at a 6 db/octave rate beyond ω_0 . It is given by¹

$$Z = \frac{R}{\exp\left(\frac{2}{\pi} \int_0^{s/\omega_0} \arctan x \frac{dx}{x}\right)} \quad (2)$$

For curve C, the phase response is linear up to ω_0 and remains at $-\pi/2$ radians beyond ω_0 . Here we have²

$$Z = \frac{R}{\sqrt{1 + \left(\frac{s}{\omega_0}\right)^2} \exp\left(\frac{s}{\omega_0} \arctan \frac{\omega_0}{s}\right)} \quad (3)$$

For curve D, the phase response is linear up to ω_0 , reaching $-\pi/4$ radians, and increases to $-\pi/2$ radians beyond ω_0 . Here,

As an application of curves A and B, consider a numerical problem involving a Bode step transition.¹ The system is shown in Fig. 2. Unity transconductance amplifiers are assumed. Three of the interstage networks, Z_{RC} , consist of a 1-farad capacitor in parallel with a 1-ohm resistor. The fourth network, Z_S , is to be synthesized so as to

¹ S. Deutsch, "Synthesis of Infinite Zero-Pole Network Structures," Microwave Res. Inst., Polytechnic Inst. of Brooklyn, N. Y., R-739-59; May, 1959.

² S. Deutsch, "A General Class of Maximally-Flat Time Delay Response Ladders," Microwave Res. Inst., Polytechnic Inst. of Brooklyn, N. Y., R-773-59; September, 1959.

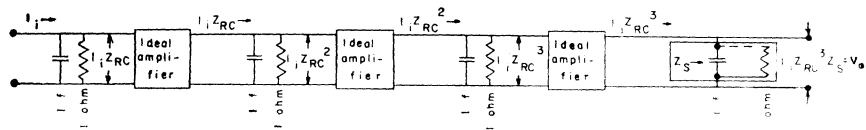


Fig. 2—The system assumed for the step transition of Fig. 3.

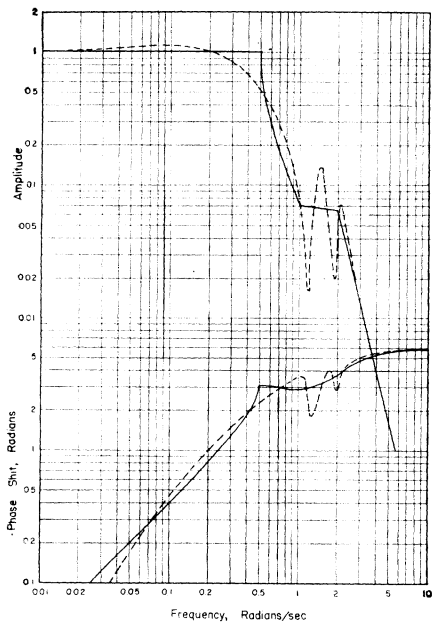


Fig. 3—Amplitude and phase responses of the step transition transfer impedance.

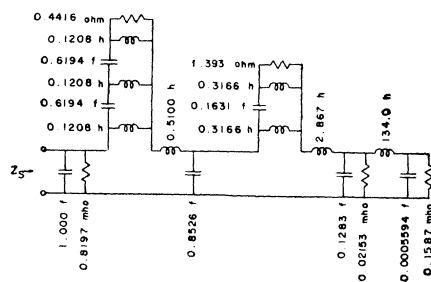


Fig. 4—The shaping network approximation for Fig. 3.

Since (7) is an infinite series, it can be realized only with an infinite number of elements. Fig. 4 shows the corresponding network approximation with 20 elements. The dotted curves in Fig. 3 show the Z_{TR} responses when the network of Fig. 4 is employed. One can approach the desired response to any degree of accuracy by carrying (7) out to additional terms and synthesizing additional elements in the network of Fig. 4.

SID DEUTSCH

Dept of Elec. Engrg.
Microwave Res. Inst.
Polytechnic Inst. of Brooklyn
Brooklyn, N. Y.

achieve a given system transfer impedance, Z_{TR} . The various impedances are related by $Z_{TR} = Z_{RC}^2 Z_S$. Two restrictions are imposed on Z_S : the first shunt element must be a 1-farad capacitor, and Z_S must approach 1 ohm as s approaches zero.

The given amplitude and phase responses of Z_{TR} are shown as the solid curves in Fig. 3. From (1) and (2), we can express Z_{TR} analytically as

$$Z_{TR} = \left[\frac{s}{0.5} + \sqrt{1 + \left(\frac{s}{0.5} \right)^2} \right]^{-2} \cdot \left[\exp \left(\frac{2}{\pi} \int_0^s \frac{\arctan x}{x} dx \right) \right]^2 \cdot \left[\exp \left(\frac{2}{\pi} \int_0^{s/2} \frac{\arctan x}{x} dx \right) \right]^{-4} \quad (5)$$

Since $Z_{RC} = 1/(s+1)$, the Z_S driving-point impedance is given by

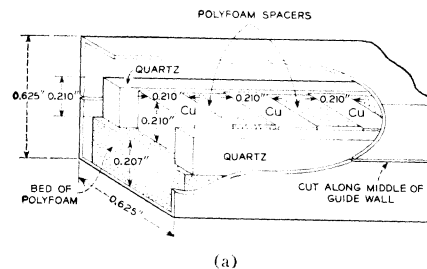
$$Z_S = Z_{TR}(s+1)^3 \quad (6)$$

When (5) and (6) are combined, the following series expansion is obtained:

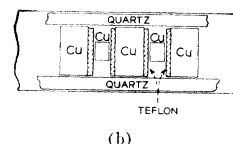
$$\frac{1}{Z_S} = s + 0.8197 + \frac{1.961}{s} - \frac{1.698}{s^2} + \frac{0.06414}{s^3} - \frac{1.674}{s^4} + \frac{5.706}{s^5} - \frac{3.960}{s^6} - \frac{2.820}{s^7} - \frac{3.388}{s^8} + \frac{22.93}{s^9} - \frac{10.27}{s^{10}} - \frac{40.41}{s^{11}} + \dots \quad (7)$$

tween blocks. The first two factors together constitute a loading capacity, and slow the wave in much the same manner as dielectric loading alone. The block spacing determines coupling between resonators, and can be made to give any arbitrary degree of slowing at the cost of a narrower bandwidth. A third mode of propagation, sketched in Fig. 2(d), may be compared with the TM_{11} mode of the empty guide, or with the mode of propagation along a coaxial line. In contrast with the latter, it has a low frequency cutoff, determined principally by the distance between blocks. The cutoff may be lowered by using a dielectric material to separate the blocks, or by placing smaller copper blocks between the large ones, as shown in Fig. 1(b). Both of these are methods of increasing the block to block capacity. In the notation used here, I and II are the slow wave modes analogous to the TE_{10} mode, and III is the mode analogous to the TM_{11} mode. Only one of the slow modes (I) was studied in the model. The other (II) was not provided with any dielectric loading, and was heavily damped by the cut along the guide wall. The magnetic fields of I and II have a component parallel to the length of the guide, and the field of III is mainly transverse.

The dimensions of the test structure are shown in Fig. 1 and correspond to cutoff frequencies in the empty guide of 9.5 kmc for the TE_{10} mode and 13.4 kmc for the TM_{11} mode. Three sizes of block were used—in the first two cases with a quartz dielectric, and in the last case with a stack of mica strips



(a)



(b)

Fig. 1.

The Block Loaded Guide as a Slow Wave Structure*

Fig. 1 shows a square cross-section wave guide cut into two U-shaped parts along the center line of two opposite walls, and loaded with small copper blocks and dielectric. The blocks rest on a bed of polyfoam and lie in a line along the center of the guide. They occupy a region which, in the TE_{10} modes of the empty guide, would contain the maximum electric field. Thus, they constitute a capacitive load, which is still further increased by the strips of dielectric filling the space between them and the guide wall. Individually, the blocks are resonators with fundamental frequencies below the cutoff frequency of the guide; together they form a coupled chain, and act as a slow wave circuit.

The field configuration of the slow wave resembles that of the corresponding TE_{10} wave and is sketched in Fig. 2(b). The group velocity is controlled by the size of the gaps between blocks and side walls, by the nature of the dielectric, and by the spacing be

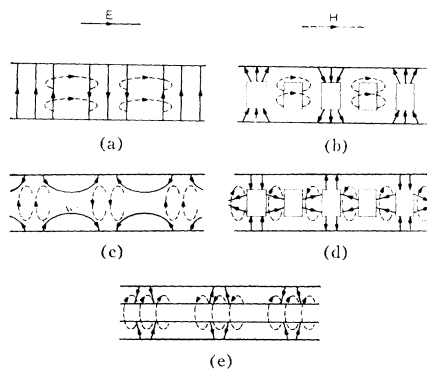


Fig. 2.

* Received by the IRE, November 25, 1959.

TABLE I

Block size	Capacity gap	Interblock spacing	Slowing factor	Mid-range frequency
0.210 inch X 0.210 inch X 0.360 inch	42 per cent	0.210 inch 0.420 inch 0.630 inch	4.6 7.0 14	5.5 kmc
0.210 inch X 0.210 inch X 0.470 inch	25 per cent	0.210 inch 0.420 inch 0.630 inch	6.3 9.5 20	4.5 kmc
0.210 inch X 0.210 inch X 0.560 inch	10 per cent	0.210 inch 0.420 inch	10 17	3.0 kmc

between the line of blocks and the side walls. Signals were coupled in and out by loops which could be rotated to make tests of the magnetic field direction. Loaded with n blocks, and lightly coupled to a power source and detector, the structure formed a multiply resonant system with n mode I resonances below the cutoff frequencies of the empty guide. In the ideal case, these give points on the dispersion curve of an infinite line;¹ in the model, there were unavoidable end effects, but tests performed, by adding a block at a time and repeating measurements, showed that five or six blocks gave a reasonable approximation. Slowing factors (free space velocity ÷ group velocity) were estimated by taking the gradient of the dispersion curve at its mid point, *i.e.*, where the blocks form $\frac{1}{4}\lambda$ sections, and where the slowing factor has a stationary minimum value. In most tests, polyfoam spacers were used between neighboring blocks, but some tests were also made with quartz spacers and with the block and teflon arrangement of Fig. 1(b). The principal effect of this change was to increase the block-to-block capacity and to bring mode III down into the mode-I range (where the two types of resonance could be distinguished by rotating the coupling loops). Mode I was hardly affected by altering the block-to-block capacity, although a small reduction in the slowing factor was noted with the Fig. 1(b) arrangement, probably because of additional electrostatic coupling between the resonating sections.

Some slowing factors for different block sizes and spacings are shown in Table I. The mid-range frequencies vary slightly with interblock spacing, and the values given are only approximate. "Capacity gap" denotes twice the distance between a block face and the side wall, expressed as a percentage of the total wall-to-wall distance. Blocks were spaced from the side walls with quartz or mica, and from one another with polyfoam.

At many of the resonances, Q -values in excess of 1000, corresponding to a loss of under $\frac{1}{2}$ db per meter at a slowing factor of 20, were obtained. This low loss is probably explained by the absence of metal-to-metal joints in the structure. It should be possible to obtain larger slowing factors by substituting strips of Al_2O_3 ceramic ($k \sim 10$) or TiO_2 ceramic ($k \sim 80$) for the quartz.

In general, the block and dielectric loaded guide is distinguished by low loss, versatility of design, and ease of construc-

tion; and it should be particularly appropriate where strong coupling with the magnetic, rather than with the electric, field is required. It may be noted that, in the test model, the region of strong electric field was filled with material, but the region of strong magnetic field (altogether $\frac{2}{3}$ of the volume) was free. As a traveling-wave maser structure it would have some special advantages. With mode I as the signal and mode III as the pump, the two H fields would be mutually perpendicular, and would overlap in the empty spaces above and below the block and dielectric strip. An external dc field applied at right angles to the length of the guide would be perpendicular to the signal field, and could have various orientations with respect to the pump. The characteristics of modes I and III can be determined with a certain amount of mutual independence, and mode III can be set beyond the mode I range, so that no fraction of the signal is coupled into the incorrect mode. Capacitative loading slows the wave, without a corresponding narrowing of the pass band. It reduces the cross section as well as the length of the structure, thus simplifying the problem of mounting in a strong magnetic field at low temperatures, and also making it possible to obtain a good filling factor, with economy in the amount of paramagnetic material and in the pumping power needed to keep it continually activated.

W. B. MIMS
Bell Telephone Labs., Inc.
Murray Hill, N. J.

Reduction of Sidelobe Level and Beamwidth for Receiving Antennas*

In the conventional application of the Dolph-Tchebycheff technique¹ an array of $N+1$, isotropic, in-phase radiators, spaced $\lambda/2$ apart, yields an optimized relationship between the beamwidth and sidelobe level of the antenna pattern, provided the method of combining the signals from the individual elements is the usual simple one. The weighting coefficient for each element is determined by the correspondence required between the antenna pattern $T_N(u)$ (where $u = \sin \theta$ and θ is measured from broadside), and the Tchebycheff polynomial, $T_N(x)$, of degree N .

* Received by the IRE, November 20, 1959.

¹ C. L. Dolph, "A current distribution for broadside arrays which optimizes the relationship between beam width and side lobe level," Proc. IRE, vol. 34, pp. 345-348; June, 1946.

It will be shown that if a slightly more complicated system behind the antenna is used, then an antenna pattern corresponding to T_{2N} may be obtained *on receive*. Fundamentally, the method consists of utilizing the identity:²

$$\frac{1}{2} T_{2N}(x) = \left(T_N(x) + \frac{1}{\sqrt{2}} \right) \left(T_N(x) - \frac{1}{\sqrt{2}} \right). \quad (1)$$

Certain features of this new technique are similar to those used in a scheme³ for improving two-way patterns.

Fig. 1 shows a schematic drawing for the case of a nineteen-element array. The term $e_1(u, t)$ denotes the RF signal which results when signals are combined from the individual elements in the conventional Dolph-Tchebycheff manner. In addition, the center element is tapped so as to yield two equal RF signals, e_2 and e_3 . The three channels are then combined as shown in Fig. 1. The complete expression for the voltage in each branch of the device is given in Table I.

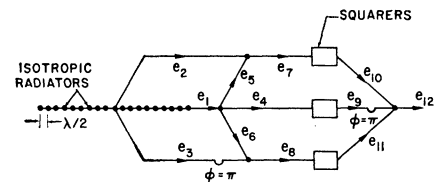


Fig. 1—Diagram illustrating new technique for reduction of sidelobe level and beamwidth for receiving antennas.

TABLE I
VOLTAGE IN EACH BRANCH OF ANTENNA
SHOWN IN FIG. 1

$e_1(u, t) = \sqrt{6} T_{18}(u) \cos \omega t$
$e_2(u, t) = (1/\sqrt{2}) \cos \omega t$
$e_3(u, t) = (1/\sqrt{2}) \cos \omega t$
$e_4(u, t) = 2T_{18}(u) \cos \omega t$
$e_5(u, t) = T_{18}(u) \cos \omega t$
$e_6(u, t) = T_{18}(u) \cos \omega t$
$e_7(u, t) \equiv e_5 + e_2 = (T_{18}(u) + 1/\sqrt{2}) \cos \omega t$
$e_8(u, t) \equiv e_6 - e_3 = (T_{18}(u) - 1/\sqrt{2}) \cos \omega t$
$e_9(u, t) = 4T_{18}^2(u) \cos^2 \omega t = 2T_{18}^2(u)(\cos 2\omega t + 1)$
$e_{10}(u, t) = (T_{18}(u) + 1/\sqrt{2})^2 \cos^2 \omega t = (1/2)(T_{18}^2(u) + \sqrt{2} T_{18}(u) + 1/2)(\cos 2\omega t + 1)$
$e_{11}(u, t) = (T_{18}(u) - 1/\sqrt{2})^2 \cos^2 \omega t = (1/2)(T_{18}^2(u) - \sqrt{2} T_{18}(u) + 1/2)(\cos 2\omega t + 1)$
$e_{12}(u, t) = e_{10} + e_{11} - e_9 = (T_{18}^2 - 1/2)(\cos 2\omega t + 1) = (1/2)T_{36} \cos 2\omega t + (1/2)T_{36}$

The output $e_{12}(u, t)$ thus corresponds to a Tchebycheff polynomial of degree 36. In principle either the time-varying or the direct current component of e_{12} may be detected.

² Tables of Chebyshev Polynomials $S_n(x)$ and $C_n(x)$, NBS Appl. Math. Ser. 9, U. S. Govt. Printing Office, Washington, D. C.; December, 1952.

³ R. L. Mattingly, Bell Telephone Labs., Private Communication; July, 1959.

¹ D. A. Watkins, "Topics in Electromagnetic Theory," John Wiley and Sons, Inc., New York, N. Y., pp. 9-10; 1958.

Characteristics of this antenna are compared to those of several conventional arrays in Table II. Because of the lack of a unique basis for comparison of this new technique and the conventional Dolph-Tchebycheff technique, the cases below were computed. The results of the application of this new technique are listed in row one.

TABLE II
PATTERN CHARACTERISTICS

Case No.	Signal Combination Method	No. of Elements	Full Beamwidth	Sidelobe Level
1	New technique	19	10.7°	-19 db
2	Conventional	19	12.0°	-16 db
3	Conventional	19	13.3°	-19 db
4	Conventional	19	10.7°	-12.5 db

If it is required that the new and conventional techniques yield the same beamwidth, then comparison of cases 1 and 4 shows that the new technique yields sidelobes which,

theoretically, are better by 6½ db. If the sidelobe level is the primary consideration, then

$$\frac{1}{2} T_{4N} = 4 \left[\left(T_N + \frac{1}{\sqrt{2}} \right) \left(T_N - \frac{1}{\sqrt{2}} \right) + \frac{1}{\sqrt{8}} \right] \cdot \left[\left(T_N + \frac{1}{\sqrt{2}} \right) \left(T_N - \frac{1}{\sqrt{2}} \right) - \frac{1}{\sqrt{8}} \right]. \quad (2)$$

cases 1 and 3 show that the new technique yields a full beamwidth which is better by 2.6°. The set of weighting coefficients for cases 1 and 2 are equal except for the center element. In this last comparison the new technique yields an improvement in full beamwidth of 1.3° and the sidelobe level is improved by 3 db.

These improvements of the conventional Dolph-Tchebycheff pattern are effected at the cost of decreasing the effective one-way range by about 25 per cent. In applications where power is abundant and high discrimination is desired, this new technique could be cascaded with still further improvements in the pattern. For example, the next

step in the cascade would make use of the identity:

A new technique which improves the conventional Dolph-Tchebycheff antenna pattern has been presented. It has been shown that the beamwidth and the sidelobe level may be reduced at the cost of increasing the complexity of the components behind the antenna and by allowing a decrease in the effective range.

The new technique is applicable only for receiving antennas. The nonreciprocity is due to the use of nonlinear detectors as an integral part of the scheme.

OLIVER R. PRICE
Microwave Lab.
Hughes Aircraft Co.
Culver City, Calif.

Contributors

Edward W. Allen (M'44-F'53) was born in Portsmouth, Va., on February 14, 1903. He received the E.E. degree from the University of Virginia, Charlottesville, in 1925, and the L.L.B. degree from George Washington University, Washington, D. C., in 1933.



E. W. ALLEN

Joining the Federal Communications Commission in 1935, he became chief of its Technical Research Division in 1946. Since 1951, he has been Chief Engineer of the FCC; and, throughout his association with the Agency, he has been active in the development of technical standards and radio allocations. A member of the Electrical Standards Board of the American Standards Association, he has participated in electrical coordination work for many years.

Mr. Allen is also a member of the national committees of URSI and of the International Electrotechnical Union.



W. L. Behrend (M'48-SM'53) was born on January 11, 1923, in Wisconsin Rapids, Wis. He received the B.S. and M.S. degrees

in 1946 and 1947, respectively, both from the University of Wisconsin, Madison.

From 1944 to 1946, he served as an electronic technician in the U. S. Navy. In 1947, he joined the RCA Laboratories Division, Princeton, N. J., where he is now with the Systems Research Laboratory. He has been associated with the development of antennas, experimental UHF television transmitter, and color television.



W. L. BEHREND

Mr. Behrend is a member of Sigma Xi.



Robert M. Bowie (A'34-M'37-SM'43-F'48) was born in Table Rock, Neb., on August 24, 1906. He received the B.S. degree in chemistry, and the M.S. and Ph.D. degrees in physics in 1929, 1931, and 1933, respectively from Iowa State University, Ames.

In 1933, he joined the engineering staff of Hygrade Sylvania Corporation, Emporium, Pa., to do physical research on radio tubes. In 1934, he began the establishment of a physical research laboratory, and in 1935, the laboratory was expanded with principal emphasis on television tube re-

search. In 1939, this laboratory was split into two parts and he continued as head of the Research Department; the other part subsequently became the Picture Tube Division. In 1940, the Research Department undertook fundamental research in electronics and spectroscopy. This work was continued until 1941, when fundamental research was put aside in order that the activities of the staff might be devoted to war research. He was responsible for the establishment of the Physics Laboratory, Sylvania Electric Products Inc., Bayside, N. Y., and in 1944, became Manager of that laboratory. He has held several titles since that date, including that of Director of Engineering from 1951 to 1955, Director of Research from 1955-1958, and Vice-President of the Sylvania Research Laboratories from 1958 to 1959. In 1960, these laboratories became the General Telephone & Electronics Laboratories Incorporated, a subsidiary of General Telephone & Electronics Corporation. Dr. Bowie is Vice-President and General Manager of the Laboratories at Bayside.



R. M. BOWIE

He has made significant contributions to vacuum tube and television research, was